Pathology (December 2012) **44(7)**, pp. 654–675

CORRESPONDENCE

Calibration of doxycycline for use in urinary tract infections with enterococci

Sir,

Enterococci are not the most common cause of urinary tract infections (UTIs) but when they do cause UTIs they present a therapeutic challenge, especially with patients who are suspected of being allergic to penicillin and cannot be treated with amoxicillin. The alternative oral agent, nitrofurantoin, has unpleasant side effects, particularly nausea and vomiting.[1] The use of other agents such as linezolid, quinupristin/dalfopristin, vancomycin and tigecycline is not justified except in the seriously ill patient.[2] Doxycycline is an oral antibiotic that is generally well tolerated and previously has been reported to have some clinical success in treating patients with UTIs.[3]

Recently we reported the calibration of tetracycline and *Enterococcus* species for treatment of systemic infections using a 10 μg disc of tetracycline hydrochloride as the surrogate disc for all tetracyclines including doxycycline.[4] The breakpoint for susceptible strains was ≤4 mg/L and cut-off zone size was ≥6 mm. The number of clinical isolates used in the calibration was 105 (49 *E. faecalis* and 56 *E. faecium*) and we took the opportunity to perform, at the same time, the susceptibility of these strains to doxycycline. There was complete concordance between the susceptibility to tetracycline hydrochloride and doxycycline; however, on minimum inhibitory concentration (MIC) testing doxycycline appeared to be four times more active than tetracycline hydrochloride.

A closer analysis of the data showed that only 36 (11 *E. faecalis* and 25 *E. faecium)* isolates were susceptible to tetracycline and these susceptible isolates had an MIC to doxycycline of 1 mg/L or less, whereas 95 (45 *E. faecalis* and 50 *E. faecium*) isolates had a low level of resistance to doxycycline with MICs of ≤16 mg/L. Urinary levels of well over this figure are achieved on oral therapeutic doses of doxycycline.[3] In addition, enterococci are rarely invasive and as a rule do not spread into the adventitial tissues.[3] Together, these observations suggest that doxycycline might be a useful urinary antiseptic for enterococcal UTI and it would be worthwhile to develop a disc test to identify those strains with MICs of ≤16 mg/L.

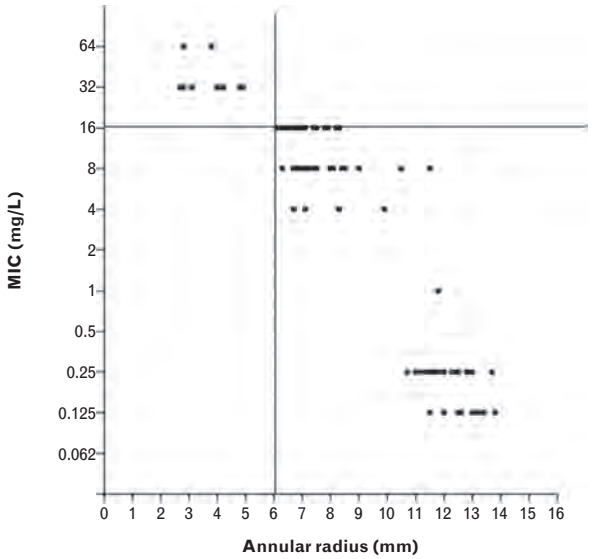

Fig. 1 Calibration of doxycycline with enterococci using a 60 μg antibiotic disc.

Calculations using the formulae proposed by Humphrey and Lightbown[5] indicated that 60 μg would be the appropriate disc to yield an annular radius of ≥6 mm for strains with an MIC of ≤16 mg/L. As commercial discs of this potency are not yet available, 60 μg discs were prepared by loading a sterile 6 mm paper disc (cat. no. 2017-006; Whatman, UK) with 25 μL of an aqueous solution of doxycycline 2400 mg/L.The discs were stored in a sterile Petri dish and used on the day of preparation. The potency of the discs was validated using the 105 isolates referred to above, by comparison, in duplicate, of the annular radii observed with the prepared discs and those observed with two stacked 30 μg commercial discs moistened with 50 μL of water. The zone sizes with the two types of discs were similar with a variation of 0.1 mm or less when measured with vernier calipers. The calibration graph with doxycycline 60 μg (Fig. 1) demonstrates a satisfactory separation of strains at the break point of ≤16 mg/L with an annular radius of ≥6 mm.

At the same time the 105 isolates were used to calibrate the commercially available 30 μg doxycycline discs (CT0018B; Oxoid, UK). A similar calibration graph was obtained to that shown, except that at a breakpoint of ≤16 mg/L the annular radius was ≥4 mm. Until commercially prepared 60 μg disc are available, a 30 μg disc may be used and will yield similar results except that the cut-off annular radius is ≥4 mm.

It is emphasised that the disc testing with doxycycline to demonstrate low-level resistance with enterococci is restricted to urinary isolates. Further, the test is an *in vitro* guide only and clinical studies are required to confirm the efficacy of doxycycline in UTIs caused by enterococci.

Conflicts of interest and sources of funding: The authors state that there are no conflicts of interest to disclose.

Sydney Bell
Jeanette Pham
Jawad Saab
Thanh Nguyen

Department of Microbiology South Eastern Area Laboratory Services, Randwick, NSW, Australia

Contact Professor S. M. Bell.
E-mail: smbell@unsw.edu.au

1. Koch-Weser J, Sidel V, Dextter M, Parish C, Finer DC, Kanarek P. Adverse reactions to sulfisoxazole, sulfamethoxazole, and nitrofurantoin. *Arch Intern Med* 1971; 128: 399.
2. Lin E, Bhusal Y, Horwitz D, Shelburne S III, Trautner B. Overtreatment of enterococcal bacteriuria. *Arch Intern Med* 2012; 172: 33–8.
3. Musher D, Minuth J, Thorstainsson S, Holmes T. Effectiveness of achievable urinary concentration of tetracyclines against 'tetracycline-resistant' pathogenic bacteria. *J Infect Dis* 1975; 131 (Suppl): S40–44.
4. The CDS Reference Laboratory. The CDS Antibiotic Susceptibility Test. Newsletter 27. 1999, updated Sept 2011 (cited Feb 2012). http://web.med.unsw.edu.au/cdstest.
5. Humphrey J, Lightbown J. A general theory for plate assay of antibiotics with some practical applications. *J Gen Microbiol* 1952; 7: 129–43.

DOI: 10.1097/PAT.0b013e328359d5ff

Print ISSN 0031-3025/Online ISSN 1465-3931 © 2012 Royal College of Pathologists of Australasia

Copyright © Royal College of pathologists of Australasia. Unauthorized reproduction of this article is prohibited.

KRAS mutation analysis in a complex molecular diagnostic referral practice: the need for test redundancy

Sir,

The *KRAS* gene encodes one of the proteins in the RAS-MAPK pathway, several signalling cascades downstream of the epidermal growth factor receptor (EGFR) activation. These mutations result in constitutively activated forms of *KRAS* which are independent of EGFR activation, thus making therapeutic agents that block *EGFR*, such as cetuximab or panitumumab, ineffective.[1,2] Activating *KRAS* mutations have been described most frequently in codons 12 and 13, with a minor proportion of activating mutations described in codons 61 and 146.[3] The importance of *KRAS* mutation status in the management of patients with metastatic colorectal cancer has led to the elaboration of consensus recommendations on *KRAS* testing.[4] However, the debate on which technology platform is superior for such molecular *KRAS* testing has been widely discussed. Even in more established personalised medicine testing, such as *HER-2* in breast cancer, the paradigm is not fixed.[5] Within the context of *KRAS* testing, there are multiple technical approaches.[6] There is not a single test platform that would be able to, by itself, replicate what was perceived as the true mutation status of every sample, as a gain of analytical sensitivity is often offset by a loss of clinical sensitivity.[7,8]

This is particularly important for reference laboratories, where if the surgical specimens submitted for analysis are of suboptimal quality, a second submission or a re-biopsy may be necessary, thereby increasing the time required to obtain an actionable result.[4] In many reference laboratories, the samples received can come from numerous sources. In our reference laboratory, we handle *KRAS* mutation analysis requests from both Asian and European countries with different stages of healthcare development and unique guidelines. These may result in differences during sample handling, which may inadvertently affect the final quality of DNA preservation. Subsequently, this may affect the choice of technical platforms used for the molecular testing.

In order to prove that a certain degree of test redundancy for *KRAS* mutational analysis is required without drastic compromise on time factor, we randomly selected 46 cases that had undergone Sanger sequencing analysis: 20 samples with detectable mutation, 16 *KRAS* wild-type, and 10 that rendered unsatisfactory results. All these cases were re-tested with a Shifted Termination Assay (capillary-electrophoresis-based). The Shifted Termination Assay (STA) detection platform, which is a type of allele specific PCR, was chosen by us for this study because it was designed by the same company (*KRAS* Mutational Analysis Reagents, Applied Biosystems, USA) for use on our in-house genetic analyser (ABI 3130XL, which has been validated for diagnostic Sanger sequencing analysis), but with the potential gain of one day in the turnaround time, producing results on the same working day as the completion of DNA extraction, rather than the day after. Thus, we could potentially improve our in-house *KRAS* inconclusive analysis rates and turnaround time without having to acquire a completely new machine, a decision that comes with risks and uncertainties. This gain in turnaround time is made possible by the use of a proprietary enzyme master mix (*KRAS* Mutational Analysis Reagents, Applied Biosystems), detection primers and chemistry protocol, designed specifically to recognise mutant or wild-type target *KRAS* sequences, so as to selectively extend an *in vitro* detection primer by 1–20 nucleotides, effectively functioning as an allele specific PCR. Primer extension products of various lengths corresponding to different *KRAS* exon 2 mutations are then separated by capillary electrophoresis and detected by a fragment analysing software.

The following selected mutations in *KRAS* codon 12 and 13 are detected by the STA: p.Gly12Ser (GGT>AGT), p.Gly12Arg (GGT>CGT), p.Gly12Cys (GGT>TGT), p.Gly12Asp (GGT>GAT), p.Gly12Ala (GGT>GCT), p.Gly12Val (GGT>GTT), p.Gly13Ser (GGC>AGC), p.Gly13Arg (GGC>CGC), p.Gly13Cys (GGC>TGC), p.Gly13Asp (GGC>GAC), p.Gly13Ala (GGC>GCC) and p.Gly13Val (GGC>GTC).

Those with discrepant results were then re-tested with a home-brew, pyrosequencing method. In all cases, DNA was isolated from prepared sections of the received formalin fixed, paraffin embedded tissue with the QIAampDNA MicroKit method (Qiagen, USA), in accordance with the manufacturer's protocol. The Sanger sequencing method was carried out as described previously.[9,10] The STA method was carried out with the Applied Biosystems STA detection kit using the guidelines recommended by the manufacturer. This test covers all relevant mutants in *KRAS* exon 2 (codon 12 and 13). Finally, the pyrosequencing assay was performed according to our previously reported assay in which a 5% threshold value was chosen to define the presence of mutation.[11] Consent for this research was obtained from our institutional ethics committee.

A total of 34 of the 36 cases of successful Sanger sequencing rendered unequivocal results (20 mutants, 16 wild-type) with both the STA and pyrosequencing method; the technical concordance was of 94%. Among the two non-concordant cases, one of the discordant cases had a different mutation, while another was determined as wild-type by Sanger but unsatisfactory by the STA method. A total of eight discordant cases were tested by three platforms (Table 1). Interestingly, five of those 10 cases that were rendered unsatisfactory by Sanger sequencing, when genotyped by the STA method, had 80% consensus (4/5) with the pyrosequencing method.

Our results suggest that a degree of technical redundancy may be necessary in reference laboratories, where there is no direct quality control of the pre-analytical determinants of molecular testing such as tissue ischaemia time, fixation time or tissue processing methods. As our results suggest, the second test may not necessarily need to be run in a different platform: the STA-based kit, which was performed using the same machine as our Sanger sequencing, was able to rescue 50% of our unsatisfactory results, with diagnostic accuracies further confirmed by the third pyrosequencing method. This redundancy may have significant positive consequences in terms of therapeutic intervention, without compromises in the turnaround time.

The reasons for the apparently discordant mutation call on Sanger sequencing which showed p.Gly12Glu (GGT>GAG), and the STA which showed p.Gly12Asp (GGT>GAT) in Case 1, are two-fold. Firstly, the STA does not include a specific primer to detect the GAG allele. Secondly, the mutation is a complex mutation, as shown in the forward and reverse sequence (Fig. 1), where our initial impression of a mutant GAG allele could also be re-interpreted as a mixture of GAG and GAT alleles, or a mutant GAT allele with a co-existent polymorphism/silent mutation GGG in codon 12,

Copyright © Royal College of pathologists of Australasia. Unauthorized reproduction of this article is prohibited.

Table 1 Summary of 10 discordant cases requiring testing on all three platforms

Sample	Sanger sequencing	STA detection	Pyrosequencing	Conclusion
1	p.Gly12Glu (GGT>GAG) – complex mutation	p.Gly12Asp (GGT>GAT)	p.Gly12Asp (GGT>GAT)	STA and pyrosequencing concurred, but mutation was apparently discordant with Sanger sequencing
2	Unsatisfactory	Wild-type	Wild-type	STA and pyrosequencing concurred
3	Unsatisfactory	12 unsatisfactory; 13 wild-type	p.Gly12Asp (GGT>GAT)	Mutation only detectable on pyrosequencing
4	Wild-type	Unsatisfactory	Wild-type	Sanger sequencing and pyrosequencing concurred
5	Unsatisfactory	p.Gly13Asp (GGC>GAC)	Unsatisfactory	Mutation only detected on STA
6	Unsatisfactory	p.Gly13Asp (GGC>GAC)	p.Gly13Asp (GGC>GAC)	STA and pyrosequencing concurred
7	Unsatisfactory	p.Gly13Asp (GGC>GAC)	p.Gly13Asp (GGC>GAC)	STA and pyrosequencing concurred
8	Unsatisfactory	Wild-type	Wild-type	STA and pyrosequencing concurred

STA, Shifted Termination Assay.

which then becomes concordant with STA and pyrosequencing. Yet another interesting reason why pyrosequencing concurred with the STA but not Sanger sequencing in this case, could be explained by the design of the nucleotide dispensation order, which by altering the dispensation order (Fig. 1) of G-A-C-T-C-A-G to G-A-G-T-C-A-G in a new pyrosequencing experiment would confirm the true nature of this apparent discrepancy by showing whether the GAG allele exists. The design of the dispensation order of G-A-C-T-C-A-G was based on a review of described and known mutant *KRAS* alleles on the Catalogue of Somatic Mutations in Cancer (COSMIC) database, which did not feature the p.Gly12Glu (GGT>GAG) variant in codon 12.

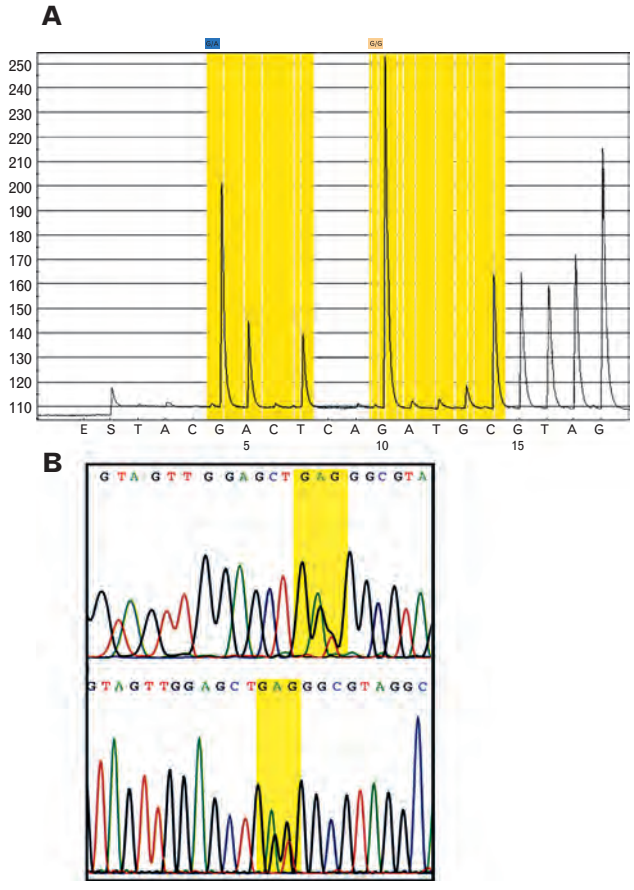

Fig. 1 (A) Pyrogram of Case 1 showing GGT>GAT mutation in codon 12 of *KRAS*. It is not possible to exclude a co-existent GGT>GAG mutation in codon 12 accounting for the tall G peak at position 10 of the horizontal axis, as the software assumes that the G peaks are read from codon 13, without re-designing the dispensation order of the nucleotides. (B) The forward and reverse Sanger sequence of the same case reveals a complex mutation in codon 12 which was initially interpreted as a heterozygous GGT>GAG, but in retrospect could also be made up of a mixture of GAG and GAT alleles, or GAT with a co-existent polymorphism/silent mutation GGG in codon 12. The STA kit does not include a primer set for detecting the GAG allele in codon 12 (not illustrated).

In conclusion, this interesting exercise shows the value of platform redundancy in revealing the composition of mutant alleles in clinical colorectal cancer samples, which resulted in an apparent discrepancy between pyrosequencing, STA and Sanger sequencing.

Conflicts of interest and sources of funding: The authors state that there are no conflicts of interest to disclose.

Brendan Pang*†
Chee-Wee Ong†
Mei-Ling Chong†
Tuty Muliana-Ismail*
Richie Soong†
Manuel Salto-Tellez*†‡

**Department of Pathology, and †Cancer Science Institute of Singapore, Yong Loo Lin School of Medicine, National University Health System, Singapore; ‡Centre for Cancer Research and Cell Biology, Queen's University Belfast, Belfast, United Kingdom*

Contact Professor M. Salto-Tellez.
E-mail: m.salto-tellez@qub.ac.uk

1. Van Cutsem E, Kohne CH, Hitre E, *et al*. Cetuximab and chemotherapy as initial treatment for metastatic colorectal cancer. *N Engl J Med* 2009; 360: 1408–17.
2. Van Cutsem E, Peeters M, Siena S, *et al*. Open-label phase III trial of panitumumab plus best supportive care compared with best supportive care alone in patients with chemotherapy-refractory metastatic colorectal cancer. *J Clin Oncol* 2007; 25: 1658–64.
3. Jimeno A, Messersmith WA, Hirsch FR, *et al*. KRAS mutations and sensitivity to epidermal growth factor receptor inhibitors in colorectal cancer: practical application of patient selection. *J Clin Oncol* 2009; 27: 1130–6.
4. Aubin F, Gill S, Burkes R, *et al*. Canadian Expert Group consensus recommendations: KRAS testing in colorectal cancer. *Curr Oncol* 2011; 18: e180–4.

Copyright © Royal College of pathologists of Australasia. Unauthorized reproduction of this article is prohibited.

5. Salto-Tellez M, Yau EX, Yan B, Fox SB. Where and by whom should gastric cancer HER2/neu status be assessed? Lessons from breast cancer. *Arch Pathol Lab Med* 2011; 135: 693–5.
6. Monzon FA, Ogino S, Hammond ME, *et al*. The role of KRAS mutation testing in the management of patients with metastatic colorectal cancer. *Arch Pathol Lab Med* 2009; 133: 1600–6.
7. Whitehall V, Tran K, Umapathy A, *et al*. A multicenter blinded study to evaluate KRAS mutation testing methodologies in the clinical setting. *J Mol Diagn* 2009; 11: 543–52.
8. Plesec TP, Hunt JL. KRAS mutation testing in colorectal cancer. *Adv Anat Pathol* 2009; 16: 196–203.
9. Krypuy M, Newnham GM, Thomas DM, *et al*. High resolution melting analysis for the rapid and sensitive detection of mutations in clinical samples: KRAS codon 12 and 13 mutations in non-small cell lung cancer. *BMC Cancer* 2006; 6: 295.
10. Pang NK, Nga ME, Chin SY, *et al*. KRAS and BRAF mutation analysis can be reliably performed on aspirated cytological specimens of metastatic colorectal carcinoma. *Cytopathology* 2011; 22: 358–64.
11. Ogino S, Kawasaki T, Brahmandam M, *et al*. Sensitive sequencing method for KRAS mutation detection by pyrosequencing. *J Mol Diagn* 2005; 7: 413–21.

DOI: 10.1097/PAT.0b013e328359d5ae

An unusual association of calcifying pseudoneoplasm of the neuraxis with interhemispheric lipoma and agenesis of corpus callosum

Sir,

Calcifying pseudoneoplasms of the neuraxis (CAPNON) are rare tumours that may occur at any place throughout the central nervous system. These lesions can be intra-axial or extra-axial and have been reported to occur in the brain and spine with similar frequency. The aetiology and natural history of these lesions are unclear. They are favoured to be non-neoplastic and reactive rather than hamartomatous or neoplastic processes. Since the original description by Rhodes and Davis in 1978,[1] there have been approximately 29 intracranial cases.[1–13] We report an unusual case of intraparenchymal CAPNON that occurred in association with interhemispheric lipoma and agenesis of corpus callosum. To our knowledge, this is the first reported association between these uncommon lesions.

A 47-year-old woman with known congenital absence of corpus callosum presented with a progressive 6 month history of worsening headache, ataxic gait, blurred vision and poor memory. She was previously cognitively normal, although there was no documented formal neuropsychological assessment. During the year prior to presentation she had noticed loss of appetite and loss of 25 kg in weight. Her laboratory investigations were unremarkable apart from elevated carcinoembryonic antigen (CEA), which was found to be 26 μg/L (normal range 0–4 μg/L). Magnetic resonance imaging (MRI) showed complete agenesis of the corpus callosum and an associated well-defined, slightly lobulated interhemispheric T1and T2 hyperintense mass $66 \times 25 \times 40$ mm consistent with a lipoma (Fig. 1A,B). In the right frontal periventricular region, anterolateral to the presumed lipoma, there was an unusual calcified intraparenchymal mass 0.9 cm in diameter. It was largely hypointense on T1 and T2 images, with intermediate signal centrally on T1, surrounded by an ill-defined vasogenic oedema (Fig. 1A,B). Differential diagnoses included a vascular lesion such as cavernoma and a neoplastic process such as metastasis.

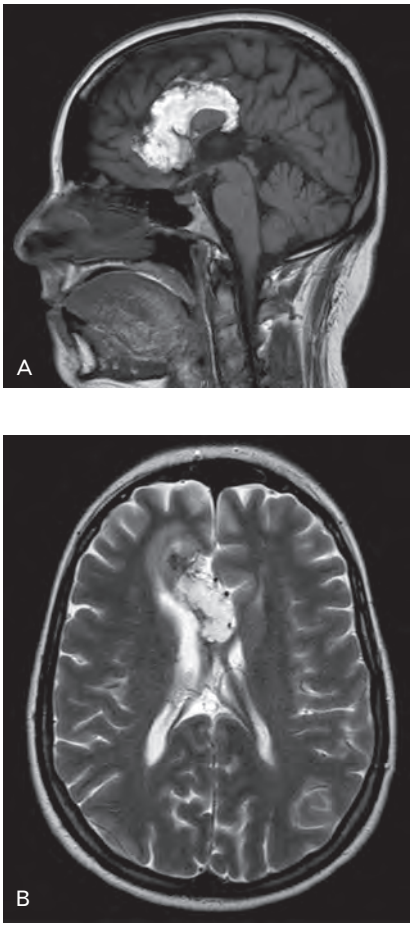

Fig. 1 MRI showed: (A) complete agenesis of the corpus callosum and an associated well-defined lobulated interhemispheric T1 hyperintense mass; (B) unusual calcified intraparenchymal mass largely hypointense on T2 in the right frontal periventricular region, anterolateral to the presumed lipoma, surrounded by an ill-defined vasogenic oedema.

The patient underwent bifrontal craniotomy and a right-sided interhemispheric approach to the lesion. Typical lipoma was identified in the midline and posteriorly. A firm calcified mass was identified anterolaterally in the right frontal lobe, which was intimately associated with one of the branches of the right callosomarginal artery. The tumour was dissected free and sent for histopathological examination.

Two specimens were received for histopathological assessment. The first specimen, labelled lipoma, consisted of multiple fragments of fatty tissue up to 3 mm across. The second, labelled right frontal lesion, consisted of multiple fragments of calcified grey/tan tissue $8 \times 7 \times 3$ mm. Microscopically, the first specimen consisted of fragments of mature adipose tissue consistent with lipoma (Fig. 2A). The second specimen revealed multiple nodules of chondromyxoid matrix (Fig. 2B), which was amorphous in places and had a prominent fibrillary pattern at the periphery of some nodules. The nodules were partially rimmed by a single layer of palisading spindled to epithelioid cells (Fig. 2C). They were set in a reactive fibrous tissue with variable and generally mild lymphocytic inflammation, and there was also prominent osseous metaplasia with focal formation of mature lamellar bone (Fig. 2D). There was some associated adipose tissue and scattered psammoma bodies. The adjacent brain parenchyma was gliotic

Copyright © Royal College of pathologists of Australasia. Unauthorized reproduction of this article is prohibited.

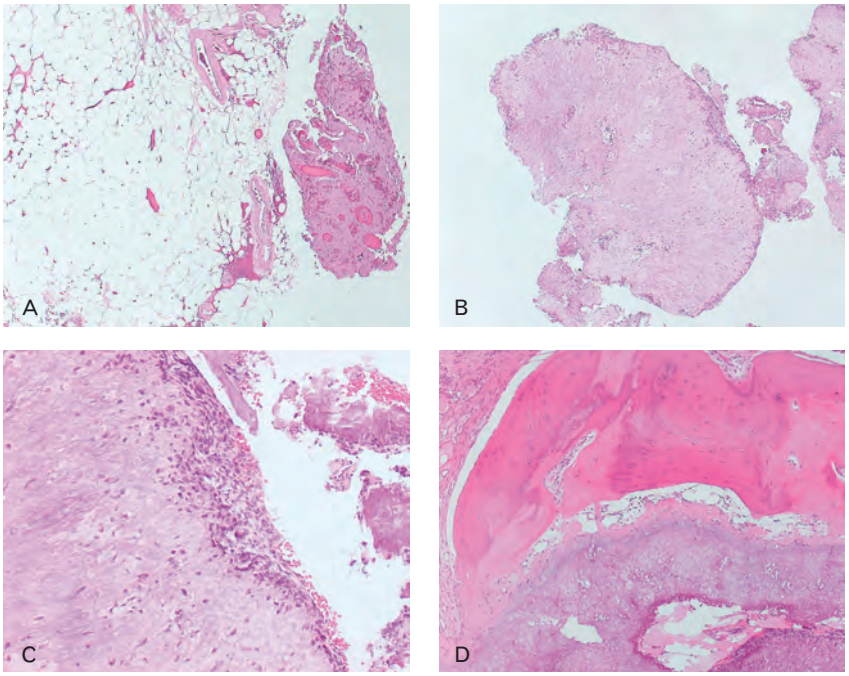

Fig. 2 H&E stained sections of the resected tumour showed (A) fragments of mature adipose tissue consistent with lipoma; (B) nodules of chondromyxoid matrix with a distinctive fibrillary pattern in areas; (C) the nodules were partially rimmed by a single layer of palisaded spindled to epithelioid cells; (D) osseous metaplasia with focal formation of mature lamellar bone.

and included a focus of piloid gliosis with Rosenthal fibres. Immunohistochemistry demonstrated patchy weak positivity for epithelial membrane antigen by the peripheral epithelioid to spindle cells with negative glial fibrillary acidic protein and S100. The final histological diagnosis was CAPNON. The patient tolerated the procedure well with no new post-operative deficits.

CAPNON are rare lesions with less than 30 cases reported in the literature. There is no reported predilection for sex, age, or CNS location. Patient age at presentation ranges from 6 to 83 years.[2] Most examples are sporadic, but CNS examples may occur in association with meningioangiomatosis in patients with neurofibromatosis type 2.[14]

The radiological features of these lesions are non-specific and can have a broad differential diagnosis, which include intra-axial calcifying neoplasms such as ganglioglioma and oligodendroglioma, vascular lesions such as cavernous malformation, and infections such as tuberculosis. Intraventricular masses can also raise the possibility of choroid plexus tumours, meningioma or ependymal tumours. The MRI imaging scans typically demonstrate hypointense signal intensity in both T1- and T2-weighted images. Vasogenic oedema is uncommon. Computed tomography (CT) images show solid attenuated calcifications.[2] The small series reported by Aiken *et al.* suggests that the uniform T1 and T2 hypointensity without solid enhancement is a key distinguishing feature.[2] Calcified lesions with heterogeneous T2 signal intensity or T2 hyperintensity are more likely to be a calcified neoplasm and radiologically inconsistent with CAPNON.[2]

The histopathological features of CAPNON are distinctive. They include characteristic nodules of chondromyxoid matrix with an amorphous granular quality centrally and fibrillary pattern at the periphery. The foci are rimmed by palisaded spindled to epithelioid cells, set in a reactive fibrous stroma with a variable lymphocytic infiltrate. There may also be a foreign body reaction with giant cells, prominent osseous metaplasia, formation of mature lamellar bone, and/or scattered psammoma bodies. The adjacent brain parenchyma usually shows gliosis with scattered Rosenthal fibres.

The pathogenesis of this lesion is not understood, but many authors have hypothesised that CAPNON is most likely a reactive process.[9,10] This is partly based on the finding of associated granulomatous inflammation typically surrounding the calcified nodules, characteristic of these lesions.[4,9,12] It has been suggested, but not proven, that CAPNON may develop as a healing response to possible trauma, infection, or inflammation.[2] The tissue origin most likely includes the arachnoid or fibroblasts in the choroid plexus stroma, but this has not been proven.[1]

The lesion reported here occurred in association with agenesis of the corpus callosum and interhemispheric lipoma. Intracranial lipomas (ICL) are rare lesions with an incidence of 0.06–0.3% of intracranial masses found during imaging.[15,16] They represent a group of congenital malformation of the brain parenchyma, mainly occurring in the region of the corpus callosum. According to the current World Health Organization classification, they are considered grade I mesenchymal, non-meningothelial tumours.[17] ICL are usually asymptomatic, although several reports mention seizures as an associated or presenting feature. The development of corpus callosum takes place from anterior to posterior with successive formation of the genu, rostrum, body and splenium, and depending on the time of injury during pregnancy, the anomalies vary from complete to partial agenesis.[16] A possible pathophysiological explanation of the association of cerebral lipoma with agenises of corpus callosum is the persistence of meninx at the site of lamina reuniens, interfering with the formation of the massa comissuralis.[18] Depending on the timing when this process occurs, the corpus callosum may not develop at all.[18]

From our review of the literature, this is the first reported case of CAPNON to occur in association with intracranial lipoma and agenesis of corpus callosum, or indeed with either

Copyright © Royal College of pathologists of Australasia. Unauthorized reproduction of this article is prohibited.

of these entities. The contiguous occurrence of this lesion with the interhemispheric lipoma may further confirm that this lesion is likely the result of a tumefactive, reactive process. In addition, the clinical presentation of our patient, which included headache, ataxic gait and blurred vision has been reported previously. However the weight loss and rising CEA levels have not been reported in other cases of CAPNON in the literature, and are currently still being investigated. Excision of CAPNON is generally curative, but may not be possible in large lesions secondarily involving vessels and nerves. Local recurrences have been described,[4,19] typically following incomplete excision.

In conclusion, CAPNON are rare distinctive lesions that can occur as extra- or intra-axial masses. Although the cause and pathogenesis are unclear, the distinctive histopathological appearance will usually lead to a definitive diagnosis of a radiologically non-specific lesion.[9] To our knowledge, this is the first reported case of CAPNON occurring in association with interhemispheric lipoma and agenesis of corpus callosum.

Conflicts of interest and sources of funding: The authors state that there are no conflicts of interest to disclose.

Alaa A. Salim*
Peter J. Wilson†
Ravi K. Cherukuri†
Sandra McKenzie‡
Michael E. Buckland*

**Department of Neuropathology, Royal Prince Alfred Hospital, Sydney, †Department of Neurosurgery, and ‡Department of Anatomical Pathology, Wollongong Hospital, Wollongong, NSW, Australia*

Contact Dr. A. Salim.
E-mail: alsalimalaa@gmail.com

1. Rhodes RH, Davis RL. An unusual fibro-osseous component in intracranial lesions. *Hum Pathol* 1978; 9: 309–19.
2. Aiken AH, Akgun H, Tihan T, *et al*. Calcifying pseudoneoplasms of the neuraxis: CT, MR imaging, and histologic features. *AJNR Am J Neuroradiol* 2009; 30: 1256–60.
3. Albu G, Deak G, Mencser Z, *et al*. Fibro-osseous lesion of the central nervous system. *Orv Hetil* 2001; 142: 1165–7.
4. Bertoni F, Unni KK, Dahlin DC, *et al*. Calcifying pseudoneoplasms of the neural axis. *J Neurosurg* 1990; 72: 42–8.
5. Garen PD, Powers JM, King JS, *et al*. Intracranial fibro-osseous lesion. Case report. *J Neurosurg* 1989; 70: 475–7.
6. Jun C, Burdick B. An unusual fibro-osseous lesion of the brain. Case report. *J Neurosurg* 1984; 60: 1308–11.
7. Montibeller GR, Stan AC, Krauss JK, *et al*. Calcifying pseudoneoplasm of the inferior colliculus: an unusual location for a rare tumor: case report. *Neurosurgery* 2009; 65: E1005–6.
8. Moosavi CA, Al-Nahar LA, Murphey MD, *et al*. Fibroosseous [corrected] pseudotumor of the digit: a clinicopathologic study of 43 new cases. *Ann Diagn Pathol* 2008; 12: 21–8.
9. Qian J, Rubio A, Powers JM, *et al*. Fibro-osseous lesions of the central nervous system: report of four cases and literature review. *Am J Surg Pathol* 1999; 23: 1270–5.
10. Rodriguez FJ, Scheithauer BW, Fourney DR, *et al*. Ependymoma and intraparenchymal calcifying pseudoneoplasm of the neural axis: incidental collision or unique reactive phenomenon? *Acta Neuropathol* 2008; 115: 363–6.
11. Shrier DA, Melville D, Millet D, *et al*. Fibro-osseous lesions involving the brain: MRI. *Neuroradiology* 1999; 41: 18–21.
12. Tatke M, Singh AK, Gupta V. Calcifying pseudoneoplasm of the CNS. *Br J Neurosurg* 2001; 15: 521–3.
13. Tsugu H, Fukushima T, Takeno Y. Calcifying pseudotumor of the neural axis—case report. *Neurol Med Chir (Tokyo)* 1999; 39: 762–5.
14. Donev K, Scheithauer BW. Pseudoneoplasms of the nervous system. *Arch Pathol Lab Med* 2010; 134: 404–16.
15. Fandino J, Bermudez J, Aran E. Quadrigeminal cistern and calcarine fissure lipoma: case report and review of the literature. *Neurocirugia (Astur)* 2005; 16: 173–6.
16. Popa RT, Feier D, Fufezan O, *et al*. Interhemispheric lipoma associated with agenesis of corpus callosum in an infant: case report. *Med Ultrason* 2011; 12: 249–52.
17. Louis DN, Ohgaki H, Wiestler OD, *et al*. The 2007 WHO classification of tumours of the central nervous system. *Acta Neuropathol* 2007; 114: 97–109.
18. Truwit CL, Barkovich AJ. Pathogenesis of intracranial lipoma: an MR study in 42 patients. *AJR Am J Roentgenol* 1990; 155: 855–64.
19. Chang H, Park JB, Kim KW. Intraosseous calcifying pseudotumor of the axis: a case report. *Spine (Phila Pa 1976)* 2000; 25: 1036–9.

DOI: 10.1097/PAT.0b013e32835a00ef

Küpffer cell haemophagocytosis presenting as fulminant liver failure

Sir,

Küpffer cell haemophagocytosis on liver biopsy may alert clinicians of a potential diagnosis of haemophagocytic syndrome (HPS). HPS is a severe systemic inflammatory condition characterised by activation and proliferation of T-lymphocytes and macrophages.[1] Activated macrophages, primarily within organs of the reticuloendothelial system, engulf erythrocytes, leukocytes, platelets and their precursors.[2] The diagnosis of HPS requires five of eight of the following: fever, splenomegaly, bicytopenia, hypertriglyceridaemia, hyperferritinaemia, low/absent natural killer (NK) cell activity, increased soluble CD25 levels and haemophagocytosis.[2] Establishing a diagnosis of HPS can be challenging but is critical since without proper medical treatment HPS may be fatal.[2] In this case report, we wish to illustrate a case of Küpffer cell hyperplasia and haemophagocytosis on liver biopsy which was associated with acute liver failure and an occult gallbladder carcinoma. We believe this association has never been reported.

A 52-year-old female presented to the Emergency Department with the sudden onset of painless jaundice. She had a 1 week history of nausea and vague abdominal discomfort. Her medical history was significant for a non-ST elevation myocardial infarction 2 months prior, hypertension and hyperlipidaemia. Her current medications included metoprolol, perindopril and rosuvastatin. Physical examination was unremarkable except for generalised jaundice. Vital signs were stable. An abdominal examination showed a soft, non-tender abdomen. There were no stigmata of chronic liver disease. Laboratory investigations discovered hepatic failure with bilirubin 158 μmol/L (reference value 3–17), AST 3830 U/L (15–37), ALT 1380 U/L (17–63) and ALP 1822 U/L (50–136) and renal failure with creatinine 1400 μmol/L (35–88) and urea 32 mmol/L (2.1–8.0). Her INR was 2.2 (0.9–1.2). Hepatitis A antibody and hepatitis B core antibody were non-reactive. Hepatitis C testing was not performed. Cytomegalovirus, Epstein–Barr virus and herpes simplex virus showed evidence of immunity with IgG reactivity. Screening for anti-smooth muscle antibody, anti-mitochondrial antibody, anti-parietal cell antibody and anti-nuclear antibody (ANA) were negative. Abdominal ultrasound identified a dilated common bile duct

Copyright © Royal College of pathologists of Australasia. Unauthorized reproduction of this article is prohibited.

(0.8 cm) and intrahepatic biliary dilatation. The patient was transferred to our tertiary care hospital with the presumptive diagnosis of drug induced hepatic failure within 24 h of the introduction of niacin. She had only taken one dose (1 g) of the niacin.

A transjugular liver biopsy was urgently performed and examined as a quick section. Interpretation was limited by frozen section artefacts. The biopsy showed lobular disarray with moderate mixed portal inflammation and no significant interface damage. Fibrosis and confluent hepatocyte necrosis were notably absent. There was severe cholestasis and a moderate ductular reaction. Scattered neutrophils infiltrated bile ducts. When permanent sections and special stains arrived, it became evident that the sinusoids were extensively dilated with a massive infiltration of activated CD68 positive Küpffer cells displaying haemophagocytosis (Fig. 1). These cells were initially misinterpreted as hepatocytes undergoing ballooning degeneration. Before a revised pathology report could be issued, the patient died; less than 48 h after admission to our centre.

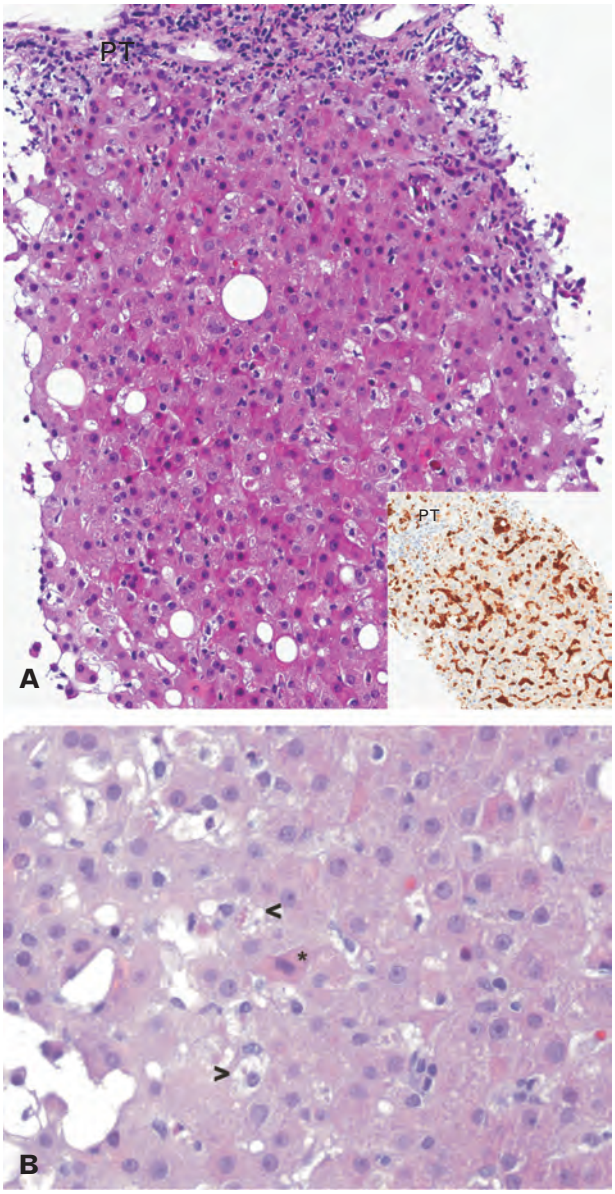

Fig. 1 Liver biopsy. (A) Massive infiltration of the sinusoids by Küpffer cells. The portal tract (PT) is indicated (H&E). Inset: CD68 positive Küpffer cells. (B) Higher power showing haemophagocytosis of erythrocytes by Küpffer cells (arrow heads) and damaged hepatocytes with acidophilic cytoplasm and clumped chromatin (asterisk) (H&E).

A post-mortem examination revealed an occult gallbladder adenocarcinoma that showed limited invasion into adjacent liver parenchyma (Fig. 2). There was metastasis to the right ovary. The poorly differentiated gallbladder adenocarcinoma had a minor signet ring component. Histological examination of the autopsy liver confirmed the presence of Küpffer cell hyperplasia and haemophagocytosis. Furthermore, mild hepatocyte ballooning degeneration and cholestasis were also noted. There was focal hepatocyte drop-out but no confluent necrosis. No centrilobular congestion or sinusoidal dilatation was seen. Congestive splenomegaly was noted (spleen weight 268 g) with significant haemophagocytosis demonstrated histologically.

The patient did not fulfil the diagnostic criteria for HPS, having only four of the required five of eight criteria,[1] including hypertriglyceridaemia (triglycerides 5.72 mmol/L; reference value 0.55–1.70), hyperferritinaemia (ferritin 50355 μ/L; 11–307), splenomegaly and haemophagocytosis. Only one cell lineage was reduced (haemoglobin 74 g/L; 115–155) instead of the required bicytopenia.

Küpffer cell haemophagocytosis is a rare observation, being detected in 1.3% of all liver biopsies.[3] However, its detection is important as it may alert clinicians to the potential diagnosis of HPS. HPS is characterised by activation and proliferation of T-lymphocytes and macrophages and by the elaboration of inflammatory cytokines.[1] Prompt treatment with immunosuppressive agents such as corticosteroids and/or cyclosporine is required in HPS to suppress the systemic inflammation.[4] It is impossible to predict whether immunosuppression in our patient would have controlled her liver failure.

Haemophagocytosis is a reactive abnormality of histiocytes that is not always associated with HPS.[5] Majluf-Cruz *et al.* found that 55% of cases with haemophagocytosis in the bone marrow, lymph node or spleen failed to develop HPS.[5] In liver biopsies with Küpffer cell hyperplasia and haemophagocytosis, 64% of cases occurred in the absence of HPS.[3] These patients had an excellent prognosis with 94% survival at 3 months. Patients with Küpffer cell haemophagocytosis and HPS had a dismal prognosis with 57% survival at 3 months.[3] Our patient demonstrated Küpffer cell haemophagocytosis without HPS,

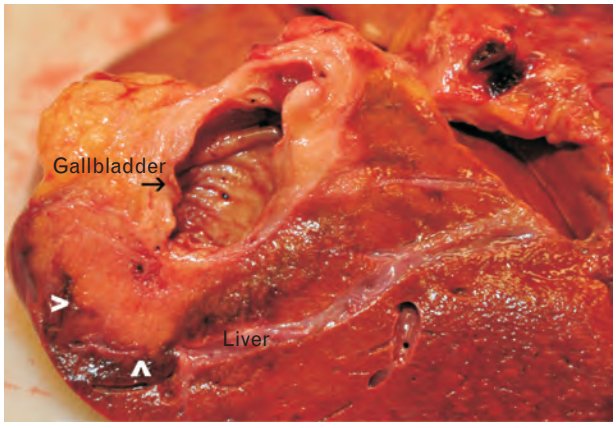

Fig. 2 At post-mortem examination, a gallbladder carcinoma was discovered with infiltration into the adjacent liver parenchyma (arrow head). Posterior view with gallbladder bisected.

Copyright © Royal College of pathologists of Australasia. Unauthorized reproduction of this article is prohibited.

yet had a rapid clinical demise. It may be that she had not fully developed all the criteria necessary for the diagnosis of HPS. Two of the diagnostic criteria for HPS, soluble CD25 levels and NK cell activity, are not routinely tested in our laboratory. Alternatively, it may be that our patient represented the 6% of individuals who die with isolated liver haemophagocytosis.

Our patient died as a result of fulminant liver failure; yet, her liver showed little morphological damage. Biliary obstruction due to gallbladder carcinoma may have contributed to the cholestatic component of liver dysfunction in this case. Other causes of acute liver failure including viruses (hepatitis A, hepatitis B, cytomegalovirus, Epstein–Barr virus and herpes simplex virus), autoimmune hepatitis, ischaemic hepatitis, thrombosis, toxins or extensive primary or metastatic tumours are excluded based on clinical history and/or laboratory investigations. There is no clinical or morphological evidence that congestive heart failure precipitated liver failure. Hepatotoxcity induced by anti-hyperlipidaemic drugs such as niacin and rosuvastatin manifest as liver necrosis or autoimmune-type hepatitis, respectively.[6] These findings were not present on the liver biopsy. Neither has been reported to induce Küpffer cell haemophagocytosis. By elimination, we believe that liver dysfunction in this case is related to massive haemophagocytosis. Since hepatocyte necrosis was present but not a prominent feature in our patient, we hypothesise that the cytokines released by activated Küpffer cells induced widespread hepatocellular dysfunction and cholestasis.[7]

Haemophagocytosis, particularly in the context of HPS, is associated with underlying conditions such as infection, malignancy or autoimmune disease.[3,8] When associated with tumours, haemophagocytosis is most commonly described with haematological malignancies.[8] This entity is rarely associated with solid neoplasms but has been demonstrated in case reports of gastric carcinoma,[9] disseminated undifferentiated ovarian carcinoma,[10] nasopharyngeal carcinoma,[10] angiosarcoma,[11] hepatocellular carcinoma,[12] mediastinal germ cell tumour,[13] and undifferentiated colon carcinoma.[14] In most of these cases, patients had clinically documented HPS with haemophagocytosis within bone marrow or lymph nodes.[9–10,12–14] Two cases described haemophagocytosis within the solid tumour.[11,14] We report a novel case of gallbladder carcinoma associated with liver haemophagocytosis.

The differential diagnosis of Küpffer cell haemophagocytosis includes large cell lymphoma and hepatic stellate cell hyperplasia which can be excluded by histology and/or immunohistochemical markers. Granulomatous hepatitis may have a similar clinical presentation, but the absence of granulomata eliminates this diagnosis.

We report a novel association between liver haemophagocytosis and gallbladder carcinoma and raise the question of a possible causal relationship between isolated liver haemophagocytosis and liver failure. The infrequent occurrence of Küpffer cell haemophagocytosis in liver biopsies highlights the need for vigilance in examining these specimens. Its recognition may alert clinicians to the challenging diagnosis of HPS and thus lead to appropriate patient management.

Conflicts of interest and sources of funding: The authors state that there are no conflicts of interest to disclose.

Allison Edgecombe*
Christopher Milroy*†
Bich N. Nguyen‡

**Department of Pathology and Laboratory Medicine, †Eastern Ontario Regional Forensic Pathology Unit, The Ottawa Hospital, Ottawa, Canada, and ‡Hôpital Saint-Luc, Centre Hospitalier de l'Université de Montréal, Montréal, Canada*

Contact Dr B. N. Nguyen.
E-mail: bnguyen.viec@gmail.com

1. Janka GE. Hemophagocytic syndromes. *Blood Rev* 2007; 21: 245–53.
2. Créput C, Galicier L, Buyse S, Azoulay E. Understanding organ dysfunction in hemophagocytic lymphohistiocytosis. *Intensive Care Med* 2008; 34: 1177–87.
3. Prendki V, Stirnemann J, Lemoine M, *et al*. Prevalence and clinical significance of Küpffer cell hyperplasia with hemophagocytosis in liver biopsies. *Am J Surg Pathol* 2011; 35: 337–45.
4. Shabbir M, Lucas J, Lazarchick J, *et al*. Secondary hemophagocytic syndrome in adults: a case series of 18 patients in a single institution and a review of literature. *Hematol Oncol* 2011; 29: 100–6.
5. Majluf-Cruz A, Sosa-Camas R, Pérez-Ramírez O, *et al*. Hemophagocytic syndrome associated with hematological neoplasias. *Leuk Res* 1998; 22: 893–8.
6. Bhardwaj SS, Chalassani N. Lipid lowering agents that cause drug-induced hepatotoxicity. *Clin Liver Dis* 2007; 11: 597–613.
7. de Kerguenec C, Hillaire S, Molinié V, *et al*. Hepatic manifestations of hemophagocytic syndrome: a study of 30 cases. *Am J Gastroenterol* 2001; 96: 852–7.
8. Imashuku S. Differential diagnosis of hemophagocytic syndrome: underlying disorders and selection of the most effective treatment. *Int J Hematol* 1997; 66: 135–51.
9. James LP, Stass SA, Peterson V, *et al*. Abnormalities of bone marrow simulating histiocytic medullary reticulosis in a patient with gastric carcinoma. *Am J Clin Pathol* 1979; 71: 600–2.
10. Chan JKC, Ng CS, Law CK, *et al*. Reactive hemophagocytic syndrome: a study of 7 fatal cases. *Pathology* 1987; 19: 43–50.
11. Dargent JL, Vermylen P, Abramowicz D, *et al*. Disseminated angiosarcoma presenting as a hemophagocytic syndrome in a renal allograft recipient. *Transpl Int* 1997; 10: 61–4.
12. Sakai T, Shiraki K, Deguchi M, *et al*. Hepatocellular carcinoma associated with hemophagocytic syndrome. *Hepatogastroenteroogy* 2001; 48: 1464–6.
13. Urban C, Lackner H, Schwinger W, *et al*. Fatal hemophagocytic syndrome as initial manifestation of a mediastinal germ cell tumor. *Med Pediatr Oncol* 2003; 40: 247–59.
14. Edgecombe AD, Nguyen BN. Focal haemophagocytosis within an undifferentiated colon carcinoma: a potential for misdiagnosis. *Pathology* 2010; 42: 304–5.

DOI: 10.1097/PAT.0b013e328359d594

Histopathological features of cutaneous drug reactions to vemurafenib: a report of two cases

Sir,

Approximately 40–60% of malignant melanomas demonstrate mutations of BRAF.[1,2] Vemurafenib (R05185426/PLX4032) is a BRAF inhibitor which is highly selective for the V600E mutation, which accounts for 90% of BRAF mutations in melanoma.[3,4] Early data from the BRIM3 clinical trial, the largest published to date, have shown improved overall and progression-free survival in patients treated with vemurafenib versus dacarbazine.[5] Development of significant side effects is common and led to dose reduction in 38% of patients on that trial. The most frequent adverse events were cutaneous, including photosensitivity, rash, alopecia and squamoproliferative lesions. The histological features of

Copyright © Royal College of pathologists of Australasia. Unauthorized reproduction of this article is prohibited.

cutaneous drug eruptions developing in patients treated with vemurafenib have not been reported. We describe the biopsy findings in two patients receiving vemurafenib for stage IV melanoma who developed cutaneous drug eruption associated with this agent.

Two cases of cutaneous drug eruption to vemurafenib were identified in a prospective study of 41 specimens from 10 patients receiving BRAF inhibitor therapy for the treatment of metastatic melanoma over a period of 15 months, from August 2010 to November 2011. This study was approved by the Sir Charles Gairdner Hospital Ethics Committee and all patients provided written informed consent for trial participation.

Case 1 was a 58-year-old man who was diagnosed with cutaneous malignant melanoma of the right thigh, Breslow thickness 1.9 mm, Clark level IV, 18 months prior to the current presentation. Initial treatment involved wide local excision of the site and selective inguinal lymph node dissection which recovered four lymph nodes, all of which contained metastatic melanoma. The patient underwent radiotherapy of the right inguinal region and 12 months of alpha interferon treatment. Four weeks prior to presentation he commenced treatment with vemurafenib at an initial dose of 960 mg twice daily. Within 2 weeks of commencement he developed multiple mucocutaneous side effects, including an erythematous macular rash, photo-onchyolysis, palmar-plantar keratoderma, bromhidrosis and uveitis. Although initially photodistributed, the skin rash became widespread, clinically showing a 'toxic erythema-like' appearance. Biopsy of affected skin from the abdomen 3 weeks after starting the drug and 1 week after symptom onset showed a subtle dermatitis, with small areas of vacuolar interface change and rare single apoptotic keratinocytes in the basal layer, but no spongiosis. A mild superficial perivascular lymphohistiocytic inflammatory infiltrate was present and occasional perivascular and interstitial eosinophils were identified (Fig. 1). The histological changes were considered consistent with an exanthematous drug reaction, and the patient was treated with topical betamethasone. The rash persisted and the patient also experienced other side effects including weight loss and anorexia. At 9 weeks post-commencement, a 1 week suspension of the drug was undertaken, followed by recommencement at a lower dose (720 mg bd). The rash improved following this and apart from one episode of minor photosensitivity 12 months later, the patient has continued on this dose for 16 months without significant recurrence. The patient has also developed multiple squamoproliferative lesions (actinic keratosis and keratoacanthoma) while on treatment. His metastatic disease has remained stable.

Case 2 was a 40-year-old man who presented to our institution with histologically confirmed metastatic malignant melanoma in the cerebellum. Further lesions were identified in the lung, subcutaneous tissues and lymph nodes of the abdomen and mediastinum. No primary cutaneous lesion was identified. He was commenced on treatment with vemurafenib 960 mg twice daily. Within 2 weeks he developed a rapid onset widespread pruritic papular eruption, originating on the lower legs and subsequently involving the upper legs, trunk, arms and neck. There were no clinical features of photosensitivity. Biopsies were taken from the right arm and left neck at routine follow-up 2 weeks later. In both biopsies orthokeratosis or minimal compact hyperkeratosis was seen overlying changes of a florid interface dermatitis. There were numerous apoptotic keratinocytes scattered throughout all levels of the epidermis, with some predominance in the basal zone, which also showed prominent vacuolar change. Focal 'satellite-cell necrosis' was noted and there were small aggregates of necrotic keratinocytes, without vesiculation or confluent epidermal death (Fig. 2A,B). A moderate superficial perivascular infiltrate was present, composed largely of lymphocytes. Once again, rare eosinophils could be identified. Notably, small foci of acantholytic dyskeratosis were noted in the biopsy from the neck (Fig. 2C). The histological appearances were considered consistent with an erythema multiforme-like pattern of cutaneous drug eruption. Topical betamethasone and wet dressings were commenced 4 weeks post-initiation of treatment. No reduction of the drug dose was undertaken in this patient. The rash persisted for a further 4 weeks, however at follow-up 11 weeks later the rash had partially resolved. The patient's metastatic disease has remained stable, with several of the metastatic lesions demonstrating reduction in size on imaging. No other skin lesions have occurred in this patient to date.

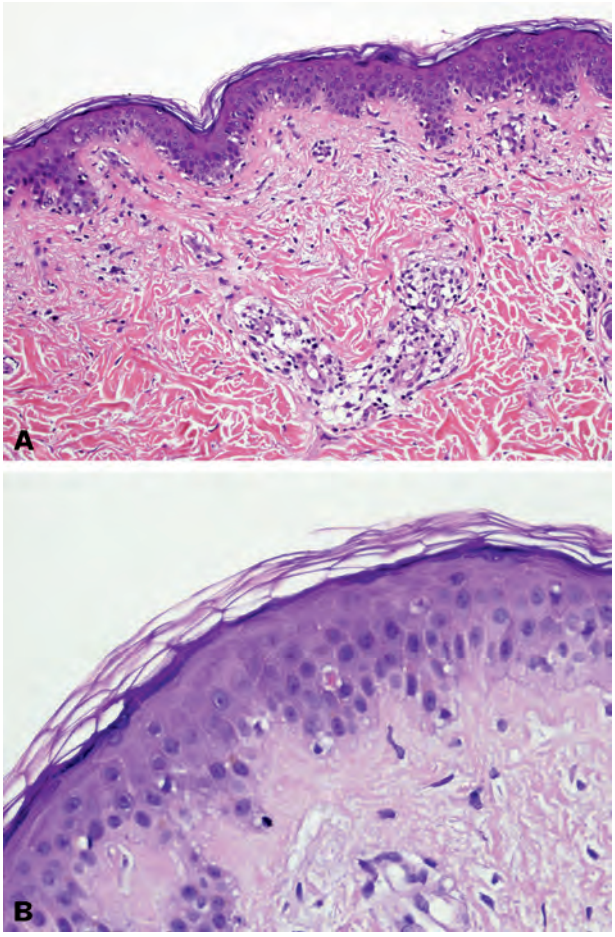

Fig. 1 Case 1, H&E. (A) Biopsy from the abdomen revealed subtle vacuolar interface change and a mild superficial perivascular lymphocytic inflammatory infiltrate. (B) Occasional single apoptotic keratinocytes were present.

Metastatic malignant melanoma has a poor prognosis.[5,6] In recent years a number of novel agents which target and inhibit the actions of mutated BRAF have been developed. These have shown mixed results in the management of such patients, with vemurafenib but not sorafenib showing evidence of improved outcome in trials to date.[5,7,8] Cutaneous adverse events associated with these drugs are commonly

Copyright © Royal College of pathologists of Australasia. Unauthorized reproduction of this article is prohibited.

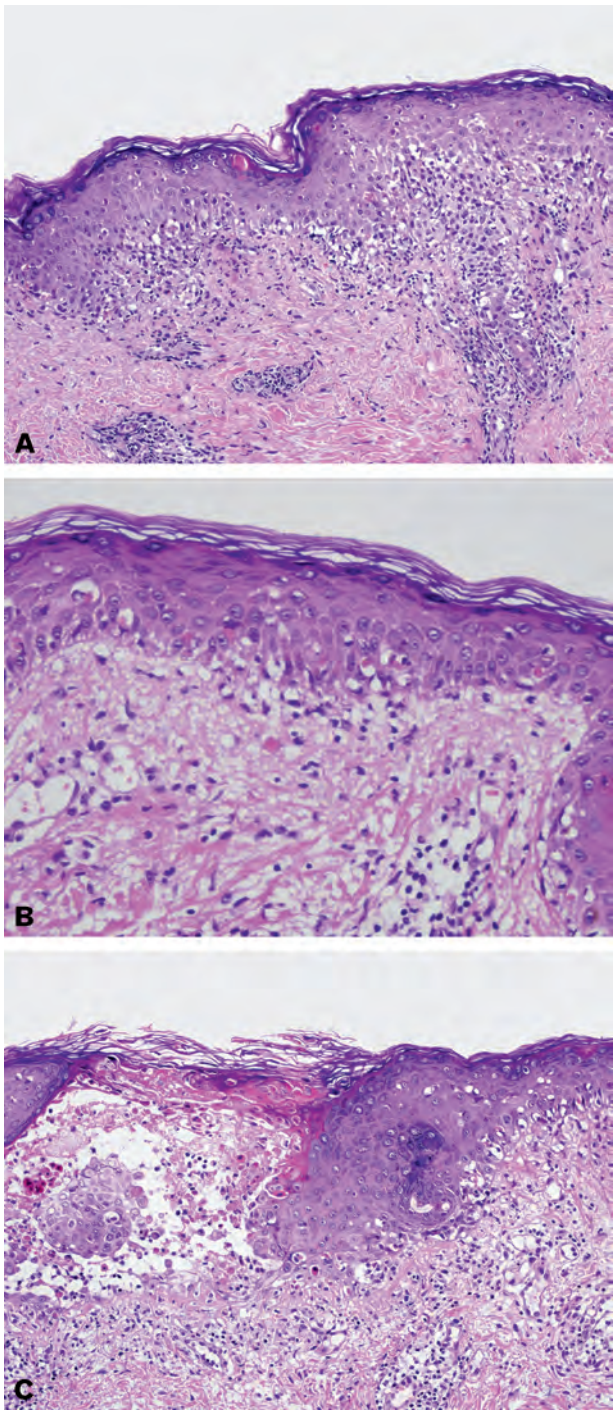

Fig. 2 Case 2, H&E. (A) Biopsies showed an erythema multiforme-like appearance, with a florid interface dermatitis and a moderate superficial perivascular inflammatory infiltrate. (B) Higher power view shows scattered apoptotic keratinocytes. (C) The biopsy from the neck showed a small focus of acantholytic dyskeratosis.

reported, including squamoproliferative lesions and cutaneous drug eruptions.[5,9,10] The clinicopathological features of non-neoplastic cutaneous side effects of BRAF inhibitors have not been well described, and to our knowledge no previous reports have documented the histological findings of cutaneous drug eruptions in response to vemurafenib.

A wide variety of inflammatory patterns can be seen in cutaneous drug eruption, and have been reviewed in detail elsewhere.[11] Lesions described clinically as exanthematous or morbilliform drug eruption account for the majority of cases in most clinical series, although the reported proportions are highly variable.[12–14] This type of reaction has been reported with a very wide array of medications, including antibiotics and antineoplastic chemotherapy among many others.[13,15,16] The histological features of this type of reaction, while subtle, are relatively characteristic, and in our clinical experience are quite strongly predictive of a drug aetiology, particularly in the setting of biopsies from hospitalised or hospital clinic patients. The histological findings in a large series of such cases were recently reviewed by Naim *et al.*[13] and are similar to those seen in Case 1. The typical pattern is of focal mild spongiosis and a mild or moderate superficial perivascular dermatitis with subtle interface change in which vacuolar alteration predominates, with occasional apoptotic keratinocytes. While eosinophils are commonly identified, they are not essential to this reaction pattern and when present are often sparse.[13,16]

The diagnosis of erythema multiforme is typically based on a combination of clinical and pathological features. Case 2 in our report showed histological features typically associated with erythema multiforme, although the clinical appearances were not those of erythema multiforme. For this reason we prefer to designate this case as an erythema multiforme-like reaction pattern on histological grounds. While the majority of cases of erythema multiforme are associated with infectious precipitants (particularly herpes simplex virus and mycoplasma infections), up to 20% may be associated with a drug aetiology.[15] The more serious clinical presentations of Stevens–Johnson syndrome and toxic epidermal necrolysis, which show significant histological overlap with erythema multiforme, are usually drug induced.[17] Typical erythema multiforme shows orthokeratosis, reflective of the acute presentation and typically short duration of lesions prior to biopsy. While our case showed some focal compact hyperkeratosis, in most areas there was orthokeratotic keratin and the other changes (scattered apoptotic keratinocytes through all levels of the epidermis and a relatively mild superficial dermal inflammatory infiltrate) were histologically typical of an erythema multiforme type reaction pattern. The histological differential diagnosis of combined interface and acantholytic reaction patterns in this case included paraneoplastic pemphigus. However, the clinical presentation was not that of paraneoplastic pemphigus,[18] mucosal lesions were absent and the eruption largely resolved with supportive care without elimination of the malignancy.

The assignation of a drug aetiology to a cutaneous eruption is frequently problematic. The wide variety of clinical and pathological presentations and large array of implicated medications can render definitive diagnosis difficult. In general terms, implication of a drug aetiology requires a history of medication ingestion, an appropriate time course for the eruption (which may vary substantially depending on the reaction type) and resolution of the lesions following medication withdrawal. While adjunctive data such as the results of rechallenge or patch testing may be helpful, they are often not available. Certain histopathological patterns are typical of cutaneous drug eruption, and in some cases a more limited correlation between a specific reaction pattern and group of causative agents can be useful in assisting diagnosis. Generally, however, histopathology is of limited value in recognising a drug aetiology, although it can be of value in excluding clinical differential diagnostic considerations. Both cases presented in this

Copyright © Royal College of pathologists of Australasia. Unauthorized reproduction of this article is prohibited.

report meet a number of criteria which lead us to consider them as bona fide examples of cutaneous drug eruption: the reactions developed within weeks of commencing a new therapeutic agent; that agent has been previously reported to result in cutaneous drug reactions clinically similar to those seen in our patients, although detailed descriptions of the histological reaction type are not yet available; in one case there was a rapid resolution of the eruption following drug dose reduction while in the other the cutaneous side effects were considered insufficiently serious to warrant dose reduction and the rash was ameliorated but not cured by topical therapy; in both cases the histological reaction pattern was one commonly associated with cutaneous drug eruption in other situations.

In most cases, management of cutaneous drug eruption includes complete withdrawal of the putative causative agent. In our patients the cutaneous reactions were considered sufficiently mild that topical treatment and in one case dose reduction rather than cessation was trialled. In both cases this was associated with remission of the symptoms. The improvement in symptoms in these patients is difficult to explain, as both reaction patterns seen in these cases are generally considered to be immunologically mediated, however this management approach and response to reduced dosage of Vemurafenib was reported in the BRIM-3 trial.[5]

We are interested in the observation that one of our cases (Case 2) showed focal acantholytic dyskeratosis. Although immunofluorescence testing was not performed, we believe that the clinical features exclude the possibility of paraneoplastic pemphigus. In reviewing a series of benign verruciform squamoproliferative lesions in patients receiving BRAF inhibitor therapy, we noted areas of acantholysis in 31%.[19] In addition, we have seen a further patient receiving BRAF inhibitor therapy who developed lesions clinically and histologically typical of Grover's disease. While these initial observations do not allow us to draw conclusions and no mechanistic explanation is established, further investigation of a possible association between pharmacological BRAF inhibition and the development of acantholysis may be worthwhile.

In summary, BRAF inhibitors represent a new class of drug that have shown early promise in treating metastatic malignant melanoma. We have described the histological features of two patients with cutaneous drug eruption associated with vemurafanib, one of the newer agents in this class, representing the first report of the microscopic findings. Both of our cases showed an interface dermatitis, with one having features typical of those seen in exanthematous type cutaneous drug eruption and the other showing features of an erythema multiforme-like reaction pattern. It is likely that continued and expanded use of vemurafanib and similar targeted therapies will result in an increased presentation of patients with cutaneous adverse reactions, and familiarity with these medications and with the histopathological findings will become increasingly important for dermatologists and pathologists.

Conflicts of interest and sources of funding: The authors state that there are no conflicts of interest to disclose.

Marcus Dabner*†
Nathan T. Harvey*†
Anita Soma*†
Benjamin A. Wood*†

**Department of Anatomical Pathology, PathWest Laboratory Medicine, QEII Medical Centre and Sir Charles Gairdner Hospital, and †School of Pathology and Laboratory Medicine, University of Western Australia, WA, Australia*

Contact Dr B. A. Wood.
E-mail: benjamin.wood@health.wa.gov.au

1. Davies H, Bignell GR, Cox C, *et al*. Mutations of the BRAF gene in human cancer. *Nature* 2002; 417: 949–54.
2. Pollock PM, Meltzer PS. A genome-based strategy uncovers frequent BRAF mutations in melanoma. *Cancer Cell* 2002; 2: 5–7.
3. Flaherty KT, McArthur G. BRAF, a target in melanoma: implications for solid tumor drug development. *Cancer* 2010; 116: 4902–13.
4. Halaban R, Zhang W, Bacchiocchi A, *et al*. PLX4032, a selective BRAF(V600E) kinase inhibitor, activates the ERK pathway and enhances cell migration and proliferation of BRAF melanoma cells. *Pigment Cell Melanoma Res* 2010; 23: 190–200.
5. Chapman PB, Hauschild A, Robert C, *et al*. Improved survival with vemurafenib in melanoma with BRAF V600E mutation. *N Engl J Med* 2011; 364: 2507–16.
6. Balch CM, Gershenwald JE, Soong SJ, *et al*. Final version of 2009 AJCC melanoma staging and classification. *J Clin Oncol* 2009; 27: 6199–206.
7. Eisen T, Ahmad T, Flaherty KT, *et al*. Sorafenib in advanced melanoma: a Phase II randomised discontinuation trial analysis. *Br J Cancer* 2006; 95: 581–6.
8. Hauschild A, Agarwala SS, Trefzer U, *et al*. Results of a phase III, randomized, placebo-controlled study of sorafenib in combination with carboplatin and paclitaxel as second-line treatment in patients with unresectable stage III or stage IV melanoma. *J Clin Oncol* 2009; 27: 2823–30.
9. Autier J, Escudier B, Wechsler J, *et al*. Prospective study of the cutaneous adverse effects of sorafenib, a novel multikinase inhibitor. *Arch Dermatol* 2008; 144: 886–92.
10. Robert C, Soria JC, Spatz A, *et al*. Cutaneous side-effects of kinase inhibitors and blocking antibodies. *Lancet Oncol* 2005; 6: 491–500.
11. Justiniano H, Berlingeri-Ramos AC, Sanchez JL. Pattern analysis of drug-induced skin diseases. *Am J Dermatopathol* 2008; 30: 352–69.
12. Crowson AN, Brown TJ, Magro CM. Progress in the understanding of the pathology and pathogenesis of cutaneous drug eruptions: implications for management. *Am J Clin Dermatol* 2003; 4: 407–28.
13. Naim M, Weyers W, Metze D. Histopathologic features of exanthematous drug eruptions of the macular and papular type. *Am J Dermatopathol* 2011; 33: 695–704.
14. Bigby M. Rates of cutaneous reactions to drugs. *Arch Dermatol* 2001; 137: 765–70.
15. Ramdial PK, Naidoo DK. Drug-induced cutaneous pathology. *J Clin Pathol* 2009; 62: 493–504.
16. Weedon D. Cutaneous drug reactions. In: Weedon D, editor. *Weedon's Skin Pathology.* 3rd ed. London: Churchill Livingstone, 2010; 514.
17. Mockenhaupt M, Viboud C, Dunant A, *et al*. Stevens-Johnson syndrome and toxic epidermal necrolysis: assessment of medication risks with emphasis on recently marketed drugs. The EuroSCAR-study. *J Invest Dermatol* 2008; 128: 35–44.
18. Horn TD, Anhalt GJ. Histologic features of paraneoplastic pemphigus. *Arch Dermatol* 1992; 128: 1091–5.
19. Harvey NT, Millward M, Wood BA. Squamoproliferative lesions arising in the setting of BRAF inhibition. *Am J Dermatopathol* 2012; Jul 5: (Epub ahead of print).

DOI: 10.1097/PAT.0b013e328359d5e2

Cellular blue naevus involving the urinary bladder

Sir,
Cellular blue naevus is an uncommon melanocytic tumour that usually arises in the skin but rarely may involve non-cutaneous sites. In this report, we present a case of cellular blue naevus involving the urinary bladder, which to the best of our knowledge is a hitherto unreported site for such a tumour.

Copyright © Royal College of pathologists of Australasia. Unauthorized reproduction of this article is prohibited.

Distinguishing features from melanoma and other relevant differential diagnoses and the role of molecular testing are considered.

A 72-year-old woman with a past history of breast cancer presented with lower abdominal pain and haematuria. Cystoscopy revealed nodules beneath the bladder mucosa. Transurethral resection (TUR) of the nodules was performed. Macroscopically, the TUR specimen consisted of multiple chips of tissue measuring 30 × 20 × 6 mm in aggregate. Microscopy showed urothelial mucosa with intact surface urothelium overlying an intravesical tumour, extending up to 5 mm beneath the surface urothelium and to the margins of the specimen. The tumour had an architectural arrangement of solid sheets and nests separated by thin fibrovascular septa with a pushing border. An associated haemangiopericytomatous-type vascular pattern was also present. There were moderate numbers of melanophages at the periphery of the tumour and around some nests. The tumour cells were oval to elongated and epithelioid with abundant pale eosinophillic cytoplasm and relatively uniform nuclei (Fig. 1). Some exhibited intranuclear longitudinal grooving. Prominent nucleoli were not a feature. No mitotic figures were identified. There was no evidence of necrosis, mucosal involvement, superficial ulceration or vascular or perineural invasion by tumour. Immunohistochemically, the tumour cells showed strong positivity for HMB45, Melan-A and weak positive staining for S100 protein (Fig. 2). The cells were negative for various keratin markers including 34βE12, CAM5.2, CK7 and CK20. CD117 was strongly positive. Desmin, smooth muscle actin, and chromogranin A were negative. The proliferation marker Ki-67 stained approximately 2% of the tumour cells (Fig. 2). Based on morphological and immunohistochemical features, a diagnosis of cellular blue naevus

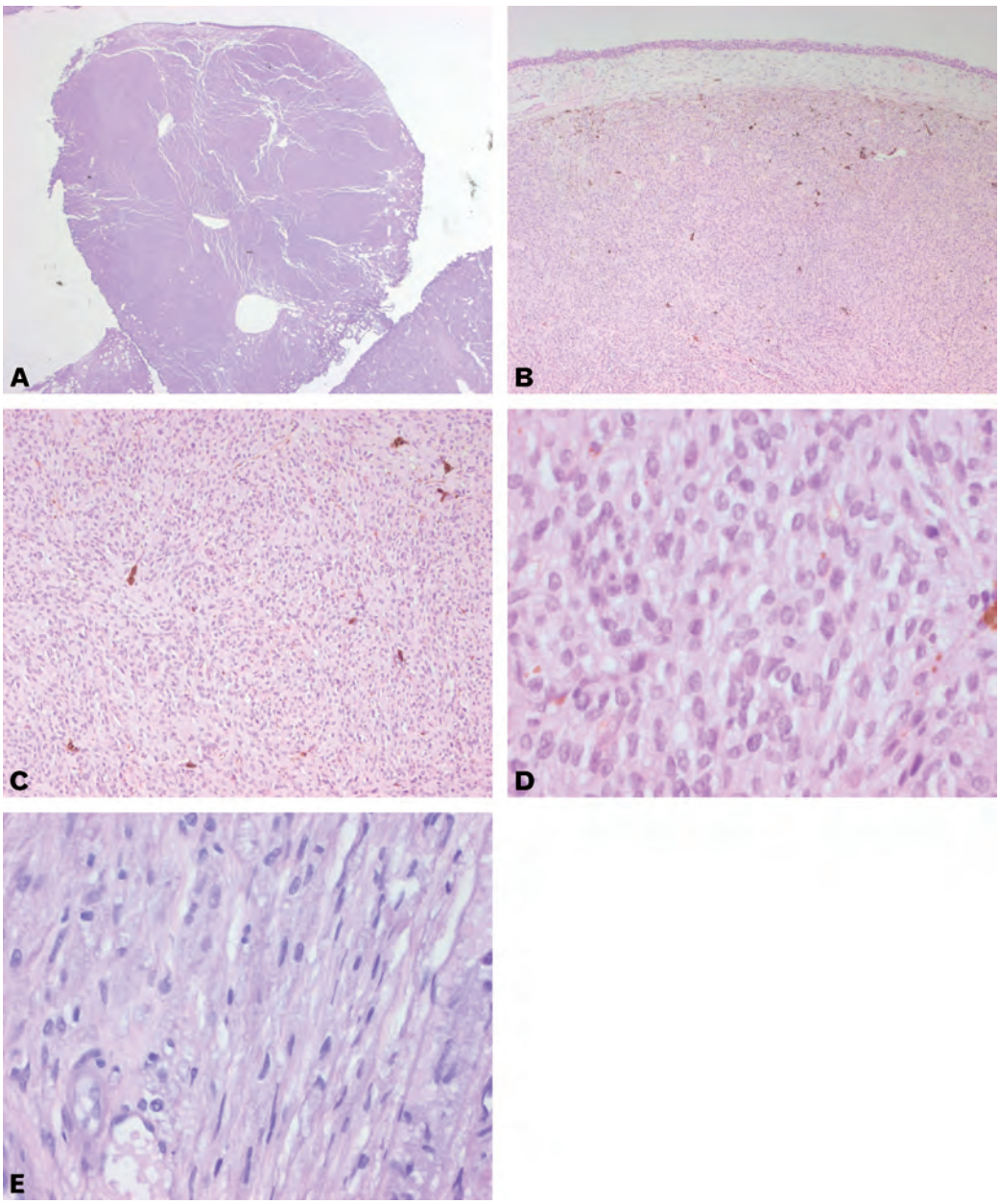

Fig. 1 Cellular blue naevus in the urinary bladder (H&E). (A,B) Low power view showing intravesical tumour with peripheral pigmentation, covered by surface urothelium. (C) The lesion shows fairly uniform cytology with paucity of mitoses and absent necrosis. (D) The cells are elongated with bland nuclei (occasionally with intranuclear longitudinal grooves) and abundant eosinophilic cytoplasm. (E) Focally the tumour includes elongated blue naevus cells with dendritic process.

Copyright © Royal College of pathologists of Australasia. Unauthorized reproduction of this article is prohibited.

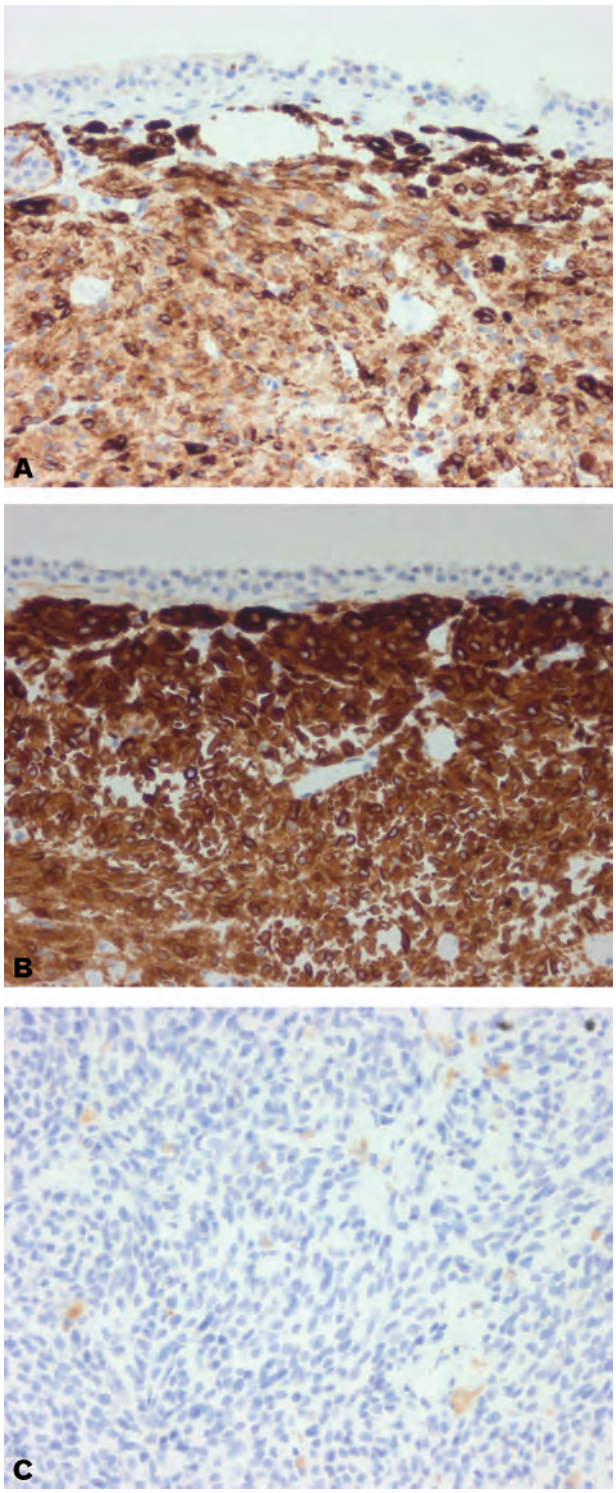

Fig. 2 Cellular blue naevus in the urinary bladder. The cells are strongly positive for S100, HMB45 (A) and Melan-A (B). (C) The proliferation marker Ki-67 stained about 2% of the lesional cells.

involving the urinary bladder was made. DNA genotyping using the MelaCARTA panel (Sequenom, USA) was performed on tumour macrodissected from the TUR specimen. This somatic mutation analysis showed a Q209L mutation in GNAQ and a G414 V mutation in PTK2B. No mutations were found in BRAF, NRAS or CKIT. These findings are consistent with a diagnosis of cellular blue naevus. A post-operative PET scan showed no evidence of residual or metastatic disease. A follow-up cystoscopy and bladder biopsy 8 months later showed a tiny amount of residual tumour with similar morphological and immunohistochemical features to the previous specimen. No evidence of recurrence or metastasis was identified 9 months later.

Blue naevi are a group of uncommon benign melanocytic tumours which are characterised by the presence of a population of spindled melanocytes with dendritic processes but may include a variety of other cells types and therefore show a diverse range of morphological appearances. It is hypothesised that blue naevi arise from immature melanocytic cells originating from the neural crest during embryonic development that become aberrantly located during their migration to the skin.[1] However, it has been shown recently that at least some blue naevi arise from schwannian cell precursors.[2] Although many variants of blue naevi have been described, the two most common histological subtypes are the dendritic (common) type and the cellular type.

The term 'cellular blue naevus' was originally coined by the eminent American pathologist Dr Arthur Allen[3] in 1949 for a 'benign variant of the blue naevus which, because of its rich cellularity and striking abundance of melanin pigment, often is misdiagnosed as melanosarcoma'. It can occur in patients of any age and either sex but the median age of diagnosis is 40 years and there is a female predominance (2.2:1).[4] The most common sites of involvement are the skin of the scalp, lower back and buttocks.[2] Uncommonly, cellular blue naevus may occur in other locations, including mucosal and subungual regions;[1,4] it has been reported to occur in the spermatic cord, prostate, uterine cervix, vagina, orbit, maxillary sinus and axillary lymph nodes.[5]

Cellular blue naevus shows a variable range of histological features, some of which may also occur in melanoma. The latter therefore represents an important potential pitfall in diagnosis. Both tumours are often characterised by dense cellularity, lack of 'maturation' with depth, deep extension, abundant pigmentation, and a range of epithelioid to spindle shaped cells.[1,4] However, there are several histological criteria that enable distinction of cellular blue naevus from melanoma in most cases (Table 1). Typically, cellular blue naevus has a uniform appearance at low power microscopy. Whilst pigment is usually fairly prominent in macrophages at the periphery of the nests of tumour cells, pigmentation within the tumour cells themselves is often light and uniform throughout the tumour. In contrast, melanoma often shows an expansile growth pattern sometimes accompanied by necrosis, with heterogenous pigmentation and an associated infiltrate of lymphoid cells. Importantly, in cellular blue naevus the cells have relatively uniform cytology with absent or low mitotic activity ($<1/mm^2$).[6] On the other hand, melanoma usually includes large epithelioid cells and shows marked nuclear pleomorphism, hyperchromasia, irregular nuclear membranes, prominent, variable and pleomorphic nucleoli and increased nuclear to cytoplasmic ratios, features which were not present in our case. Immunohistochemical stains for HMB-45, S100 and Melan-A are not helpful in distinguishing those two lesions as they both stain positively. However, Ki-67 tends to be higher in melanomas (often $>10\%$) than in cellular blue naevi (usually $<5\%$).

Atypical cellular blue naevus is a term that has been used to describe a cellular blue naevus with one or more atypical features that raise the possibility of, but are not definite for, malignancy. Whilst most lesions reported as

Copyright © Royal College of pathologists of Australasia. Unauthorized reproduction of this article is prohibited.

Table 1 Pathological differences and distinguishing features between cellular blue naevus and melanoma

Feature	Cellular blue naevus	Melanoma
Symmetry	Usually present	Often absent
Expansile growth	Absent	Often present
Cellularity	Moderately high but uniform	Often heterogenous (with marked hypercellular foci)
Pigmentation distribution	Usually uniform	Heterogeneous
Pigmentation	Predominantly in macrophages at periphery of tumour nests, light and uniform in tumour cells	Heterogeneous (may be light or heavy in tumour cells and macrophages)
Nuclear features	No/minimal atypia, minimal pleomorphism	Nuclear atypia with pleomorphism, hyperchromasia, irregular nuclear membrane, prominent nucleoli, increased N:C ratio
Junctional component	Absent (unless part of a combined naevus)	Usually present (with confluent growth and Pagetoid spread)
Necrosis	Absent	Present occasionally
Peripheral lymphoid infiltrate	Rare	Common
Mitotic activity	Rare/occasional	Present (usually $>2/mm^2$)
Ki-67 proliferative index	Low (<5%)	Increased (often >10%)
Somatic mutations	GNAQ, GNA11	BRAF, NRAS, CKIT, GNAQ, GNA11
Chromosomal aberrations	Absent/rare	Frequent

atypical cellular blue naevus have behaved clinically in a benign fashion, occasionally bonefide melanomas (resulting in metastasis and patient death) may be virtually indistinguishable histologically from benign naevi. For this reason, atypical cellular blue naevi are generally regarded as being of uncertain malignant potential, although the risk of aggressive clinical behaviour of individual tumours appears low.[6,7] Atypical histological features that may in isolation warrant a diagnosis of atypical cellular blue naevus include size >10 mm, asymmetry, hypercellular foci, cell crowding, mild nuclear hyperchromasia or pleomorphism and occasional mitoses ($<2/mm^2$).[6,7]

A study of chromosomal copy number changes in blue naevi, atypical cellular blue naevi and blue naevi-like melanomas showed no chromosomal aberrations in blue naevi, infrequent and low numbers of aberrations in atypical cellular blue naevi and more frequent aberrations in melanomas, suggesting that there are molecular changes that underpin and support the morphological classification.[8] However, a recent study revealed poor interobserver reproducibility, with substantial disagreement even among expert pathologists in the diagnosis and distinction between atypical cellular blue naevus and blue naevus-like melanoma.[9] Clearly further studies are required that combine careful morphological and molecular analysis with long-term clinical follow-up of sufficient numbers of cases to more precisely define these lesions by reproducible criteria. In the meantime, based on the limited data currently available, it would appear appropriate to treat the atypical cellular blue naevus as a lesion 'of uncertain malignant potential'.[1]

The term blue naevus-like melanoma (so-called malignant blue naevus) was coined in 1953 by Allen and Spitz to describe blue naevus-like tumours which had resulted in metastasis and patient death in some cases.[10] It is rare and usually occurs in people >45 years of age.[11] In most cases, blue naevus-like melanoma is characterised by the presence of a clearly malignant tumour occurring in association with a well recognisable cellular blue naevus.[1,4] Such features of malignancy, as described above, were absent from the current case.

It has been reported that melanoma, once it has metastasised to the skin, can simulate blue naevus.[12,13] Cutaneous metastasis of melanoma can show a spectrum of histological appearances, some of which adopt unusual morphology that mimics other benign and malignant neoplasms other than primary melanoma. Therefore, distinction of blue naevi from metastatic melanoma may be difficult in some cases. Subtle morphological features that suggest a possible diagnosis of blue naevus-like metastatic melanoma include the presence of mitoses, an associated lymphoid infiltrate and nuclear pleomorphism and hyperchromasia. Recently, it was reported that fluorescence *in situ* hybridisation (FISH) may be helpful in difficult cases.[14,15] Nevertheless, careful correlation with clinical features, including whether or not there is a past or concurrent history of melanoma occurring elsewhere, is essential for accurate diagnosis.

Several other differential diagnoses should be considered when diagnosing cellular blue naevus, particularly when occurring at an unusual anatomical location. The distinct nested growth pattern with associated melanin pigmentation, as illustrated in our case, might raise the possibility of low grade clear cell sarcoma (melanoma of soft parts) and perhaps melanotic paraganglioma. Perivascular epithelioid cell tumour (PEComa) also expresses melanocytic markers and can simulate cellular blue naevus. Clear cell sarcoma usually shows greater pleomorphism than is present in cellular blue naevus, often includes scattered tumour giant cells, has a characteristic t(12;22)(q13;q12) balanced translocation and evidence of a EWS gene rearrangement by FISH.[16] Unlike cellular blue naevus, melanotic paraganglioma has a rich vascular network surrounding the tumour nests, presence of sustentacular cells and evident of neuroendocrine differentiation morphologically and immunohistochemically. PEComas are composed of fairly uniform epithelioid cells with abundant pale granular cytoplasm and lack spindled and dendritic cells that are always present in blue naevi. Furthermore, whilst both tumours are positive for HMB45, PEComas are often negative for S100 and express smooth muscle actin, unlike cellular blue naevi.

Molecular testing, including FISH testing, is developing a role in the diagnosis of problematic melanocytic tumours and can assist in their classification.[17,18] Recently, it was revealed that a somatic mutation in the heterotrimeric G protein alpha subunit q (*GNAQ*) is often present in blue naevi of the skin (83%).[19] The mutation occurs exclusively in codon 209 and results in constitutive activation of the MAP kinase-pathway, turning GNAQ into a dominant acting

Copyright © Royal College of pathologists of Australasia. Unauthorized reproduction of this article is prohibited.

oncogene. Whilst GNAQ mutations occur frequently in uveal melanomas, they are extremely rare in cutaneous melanoma. It is unknown whether they are present in blue naevus-like melanomas, but it would appear inappropriate to exclude a diagnosis of melanoma purely on the basis of the detection of a GNAQ mutation. In contrast to blue naevi, cutaneous melanomas frequently show oncogenic mutations in BRAF and NRAS, and some mucosal and acral melanomas harbour CKIT mutations.[19] The presence of activating mutations in BRAF or CKIT in metastatic melanoma now has therapeutic implications with the recent development of effective therapies targeting them.[20]

In summary, we report a case of cellular blue naevus involving the urinary bladder, a previously unreported site. Whilst knowledge of the histopathological features of cellular blue naevus should suggest the diagnosis when it occurs in unusual anatomical sites, it may be difficult to rule out malignancy (primary or metastatic) if there are any atypical features. In such instances, complete excision, correlation with clinical features, additional investigations and careful clinical follow-up are advisable. In the future, molecular testing may provide more accurate classification of atypical cellular blue naevi.

Acknowledgements: The authors thank staff of the Department of Tissue Pathology and Diagnostic Oncology at the Royal Prince Alfred Hospital for their support and assistance.

Conflicts of interest and sources of funding: The authors state that there are no conflicts of interest to disclose.

Jennifer Kim*
Stanley W. McCarthy*†‡§
John F. Thompson‡||
Gulietta M. Pupo‡¶
Leon Vonthethoff**
Peter Nash††
Graham J. Mann‡¶
Richard A. Scolyer*†‡§

*Departments of *Tissue Pathology and Diagnostic Oncology, and †Melanoma and Surgical Oncology, Royal Prince Alfred Hospital, Camperdown, ‡Melanoma Institute Australia, Sydney, Disciplines of §Pathology, and ||Surgery, Sydney Medical School, The University of Sydney, Sydney, ¶Westmead Institute for Cancer Research, University of Sydney at the Westmead Millennium Institute, Westmead Hospital, Westmead, **Department of Anatomical Pathology, South Eastern Area Laboratory Service, and ††Department of Urology, St George Hospital, Kogarah, NSW, Australia*

Contact Dr R. A. Scolyer.
E-mail: richard.scolyer@sswahs.nsw.gov.au

1. Murali R, McCarthy SW, Scolyer RA. Blue nevi and related lesions. A Review highlighting atypical and newly described variants, distinguishing features and diagnostic pitfalls. *Adv Anat Pathol* 2009; 16: 365–82.
2. Adameyko I, Lallemend F, Aquino JB, *et al*. Schwann cell precursors from nerve innervation are a cellular origin of melanocytes in skin. *Cell* 2009; 139: 366–79.
3. Allen AC. A reorientation on the histogenesis and clinical significance of cutaneous nevi and melanomas. *Cancer* 1949; 12: 28–56.
4. Rodriguez HA, Ackerman LV. Cellular blue nevus. Clinicopathologic study of forty-five cases. *Cancer* 1968; 21: 393–405.
5. Gonzalez-Campora R, Galera-Davidson H, Vazquez-Ramirez FJ, *et al*. Blue nevus: classical types and new related entities. A differential diagnostic review. *Pathol Res Pract* 1994; 190: 627–35.
6. Temple-Camp CR, Saxe N, King H. Benign and malignant cellular blue nevus. A clinicopathological study of 30 cases. *Am J Dematopathol* 1988; 10: 289–96.
7. Tran TA, Carlson JA, Basaca PC, *et al*. Cellular blue nevus with atypia (atypical cellular blue nevus): a clinicopathologic study of nine cases. *J Cutan Pathol* 1998; 25: 252–8.
8. Maize J, McCalmont TH, Carlson JA, *et al*. Genomic analysis of blue nevi and related dermal melanocytic proliferations. *Am J Surg Pathol* 2005; 29: 1214–20.
9. Barnhill RL, Argenyi Z, Berwick M, *et al*. Atypical cellular blue nevu (cellular blue nevu with atypical features): lack of consensus for diagnosis and distinction from cellular blue nevi and malignant melanoma ('malignant blue nevus'). *Am J Surg Pathol* 2008; 32: 36–44.
10. Allen AC, Spitz S. Malignant melanoma; a clinicopathological analysis of the criteria for diagnosis and prognosis. *Cancer* 1953; 6: 1–45.
11. Martin RC, Murali R, Scolyer RA, *et al*. So-called 'malignant blue nevus': a clinicopathologic study of 23 patients. *Cancer* 2009; 115: 2949–55.
12. Busam KJ. Metastatic melanoma to the skin simulating blue nevus. *Am J Surg Pathol* 1999; 23: 276–82.
13. Wieselthier JS, White WL. Cutaneous metastasis of ocular malignant melanoma. An unusual presentation simulating blue nevi. *Am J Dermatopathol* 1996; 18: 289–95.
14. Gammon B, Busam KJ, Gerami P, *et al*. Fluorescence in situ hybridization for distinguishing cellular blue nevi from blue nevus-like melanoma. *J Cutan Pathol* 2011; 38: 335–41.
15. Pouryazdanparast P, Newman M, Gerami P, *et al*. Distinguishing epithelioid blue nevus from blue nevus-like cutaneous melanoma metastasis using fluorescence in situ hybridization. *Am J Surg Pathol* 2009; 33: 1396–400.
16. Tanas MR, Rubin BP, Goldblum JR, *et al*. Utilization of fluorescence in situ hybridization in the diagnosis of 230 mesenchymal neoplasms: an institutional experience. *Arch Pathol Lab Med* 2010; 134: 1797–803.
17. Scolyer RA, Murali R, McCarthy SW, *et al*. Histologically ambiguous ('borderline') primary cutaneous melanocytic tumors: approaches to patient management including the roles of molecular testing and sentinel lymph node biopsy. *Arch Pathol Lab Med* 2010; 134: 1770–7.
18. Morey AL, Murali R, McCarthy SW, *et al*. Diagnosis of cutaneous melanocytic tumours by four-colour fluorescence in situ hybridisation. *Pathology* 2009; 41: 383–7.
19. Van Raamsdonk CD, Bezrookove V, Green G, *et al*. Frequent somatic mutations of GNAQ in uveal melanoma and blue naevi. *Nature* 2009; 457: 599–602.
20. Scolyer RA, Long GV, Thompson JF. Evolving concepts in melanoma classification and their relevance to multidisciplinary melanoma patient care. *Mol Oncol* 2011; 5: 124–36.

DOI: 10.1097/PAT.0b013e328359e142

CD3 expression in plasma cell neoplasm (multiple myeloma): a diagnostic pitfall

Sir,

A diagnosis of plasma cell neoplasm on histology is usually straightforward. However, plasma cell neoplasms may occasionally display unusual phenotypic expression.[1] For instance, the expression of CD20 in 15–20% of plasma cell myelomas is well documented,[2] a feature which may potentially be confused with a diagnosis of B-cell lymphoma (e.g., mantle cell lymphoma when there is concomitant cyclin D1 expression) if attention is not paid to the morphological appearance. In this report, we detail an instance where the neoplasm had aberrant CD3 expression, an exceedingly rare phenomenon, resulting in a misdiagnosis of T-cell lymphoma. Interestingly, other haematolymphoid neoplasms with a

Copyright © Royal College of pathologists of Australasia. Unauthorized reproduction of this article is prohibited.

plasmacytic differentiation (plasmablastic phenotype) capable of expressing T-cell antigens such as CD3 include plasmablastic lymphoma[3] and primary effusion lymphoma.[4]

A 67-year-old man underwent an oesophagogastroduodenoscopy (OGD) for upper gastrointestinal bleeding. The OGD disclosed multiple bulbous lesions in the stomach and duodenum which were clinically suspicious for malignancy. A gastric biopsy was performed and a diagnosis of peripheral T-cell lymphoma, not otherwise specified, was initially made on light microscope examination. At around the same time, the patient developed soft tissue swelling in the right supraclavicular region, thought to represent lymphadenopathy. The mass was biopsied and the histology resembled that of a plasma cell neoplasm. In view of the discordant findings between the gastric and soft tissue biopsies, a review of both clinical and pathology findings was undertaken. Significantly, on review, the patient had a history of multiple myeloma which presented 4 years earlier affecting the left radius.

The biopsy from the OGD procedure produced three pieces of tissue from the stomach measuring 2–3 mm. On histology (Fig. 1), the small fragments of non-specialised gastric mucosa showed areas containing a diffuse infiltrate of poorly preserved medium to large discohesive cells resembling lymphoid cells in the lamina propria (Fig. 1A,B). Further morphological characterisation of the neoplastic cells was made difficult as these cells appeared poorly preserved. The tumour cells stained for CD3 (Fig. 1C) but not for CD2 and CD5 on immunohistochemistry. The stains for CD7, CD10, CD20 and granzyme B were negative. Focal staining with CD56 was present. *In situ* hybridisation for Epstein–Barr encoded RNA revealed no signals.

The biopsy from the supraclavicular region comprised two cores of tissue measuring 20 × 1 mm and 16 × 1 mm. On light microscopy, there was a diffuse infiltrate of medium to large cells with eccentric nuclei resembling plasma cells within the fibrous stroma (Fig. 2A,B). The panel of immunohistochemical stains performed revealed strong diffuse staining for CD138 (Fig. 2C) with CD56 expression. *In situ* hybridisation for light chain mRNA revealed lambda light chain restriction. A retrospective work-up on the supraclavicular tumour revealed positive CD3 expression (Fig. 2D) and negative CD2 and CD5 expressions by the neoplastic plasma cells. Similarly, a retrospective CD138 stain on the gastric tissue showed that the neoplastic cells within the lamina propria were plasma cells (Fig. 1D). Taking into account the clinical history and the overall findings on histology, the features were those of a plasma cell neoplasm (multiple myeloma) with aberrant CD3 expression.

Detection of T-cell specific antigens in neoplastic plasma cells, although extremely uncommon, has been described by Spier *et al.*[5] and the antigens expressed include CD2, CD3 and CD4, CD4 expression being the most common. In her series of 215 cases of multiple myeloma, only six cases (2.8% of cases) expressed T-cell related antigens and, interestingly, the tumour cells expressed only one T-cell related antigen each time. Only one case in her series expressed CD3. However, the expression of less specific T-cell related antigens such as CD43 and CD45RO (UCHL-1) was more frequent compared to those described above.[6] As the plasma cells disclosed aberrant CD3 expression in our case and plasma cells are by nature negative for other T-cell markers such as CD2 and CD5, this manifestation resulted in an impression of apparent aberrant loss of T-cell antigens by the tumour cells (which were thought to be T-cells initially in view of CD3 positivity) and hence a misdiagnosis of T-cell lymphoma. This case clearly emphasises the need to correlate with the clinical history, particularly in a situation similar to ours when the initial specimen showed neoplastic cells with suboptimal preservation and the phenotypic expression mimicked that of a T-cell lymphoma. Certainly, awareness of the ability of plasma cell neoplasms to express aberrant phenotypes such as T-cell antigen, careful light microscopic examination, performance of a panel of immunohistochemistry stains including plasma cell markers such

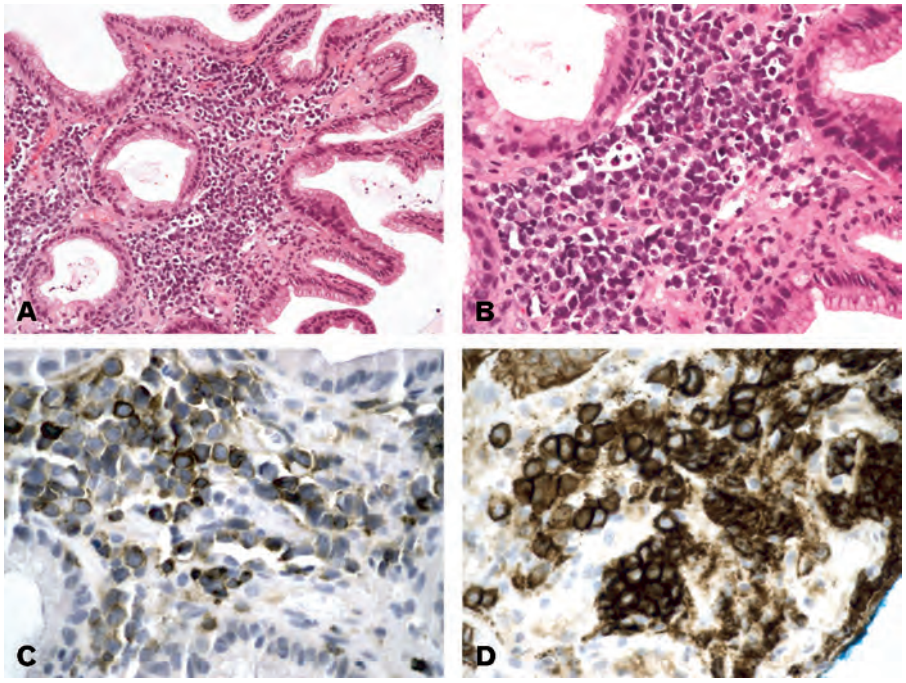

Fig. 1 (A) Medium power view of the gastric biopsy revealing an infiltrate of abnormal cells within the lamina propria (H&E). (B) High power view disclosing an infiltrate of large abnormal cells with anisonucleosis and mitotic activity resembling haematolymphoid cells (H&E). (C) Tumour cells highlighted by antibodies against CD3, mimicking a T cell lymphoma (Ventana Ultraview). (D) Retrospective immunohistochemistry stain for CD138 decorating neoplastic cells strongly and diffusely, betraying a diagnosis of plasma cell neoplasm (Ventana Ultraview).

Copyright © Royal College of pathologists of Australasia. Unauthorized reproduction of this article is prohibited.

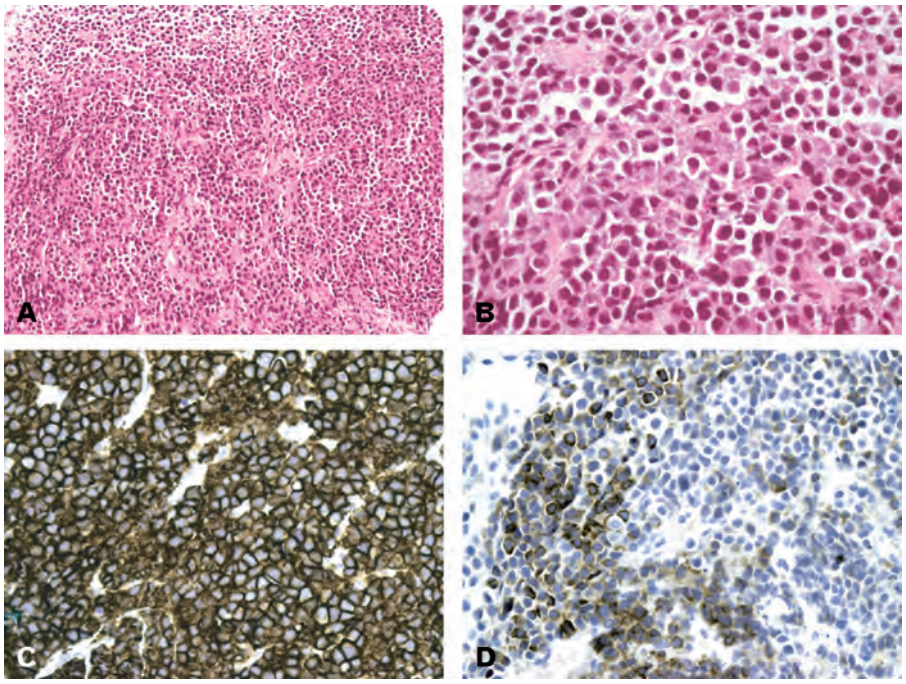

Fig. 2 (A) Medium power view of the supraclavicular soft tissue lesion revealing a cellular infiltrate of neoplastic cells separated by fibrous septae (H&E). (B) High power view showing fairly uniform cells with appreciable rim of cytoplasm and eccentric disposition of the nuclei in several areas resembling plasma cells (H&E). (C) Neoplastic plasma cells with strong and diffuse staining for CD138 (Ventana Ultraview). (D) Retrospective immunohistochemistry stain for CD3 decorating the tumour cells strongly in several areas (Ventana Ultraview).

as CD138, and better preserved tissue specimens, are pivotal in ensuring the appropriate diagnosis in problematic cases.

Conflicts of interest and sources of funding: The authors state that there are no conflicts of interest to disclose.

Yee Lin Tang
Cora Yuk-Ping Chau
Wai Ming Yap
Khoon Leong Chuah

Department of Pathology, Tan Tock Seng Hospital, Singapore

Contact Dr K. L. Chuah.
E-mail: gzzckl@singnet.com.sg

1. McKenna RW, Kyle RA, Kuehl WM, *et al*. Plasma cell neoplasms. In: Swerdlow SH, Campo E, Harris NL, Jaffe ES, editors. *WHO Classification of Tumours of Haematopoietic and Lymphoid Tissues.* Lyon: IARC Press, 2008; 201–13.
2. Quinn J, Percy L, Glassford J, *et al*. CD20-positive multiple myeloma – differential expression of cyclins D1 and D2 suggests a heterogeneous disease. *Br J Haematol* 2010; 149: 156–9.
3. Sun J, Medeiros LJ, Lin P, *et al*. Plasmablastic lymphoma involving the penis: a previously unreported location of a case with aberrant CD3 expression. *Pathology* 2011; 43: 54–7.
4. Said JW, Shintaku IP, Asou H, *et al*. Herpesvirus 8 inclusions in primary effusion lymphoma: report of a unique case with T-cell phenotype. *Arch Pathol Lab Med* 1999; 123: 257–60.
5. Spier CM, Grogan TM, Durie BG, *et al*. T-cell antigen-positive multiple myeloma. *Mod Pathol* 1990; 3: 302–7.
6. Petruch UR, Horny HP, Kaiserling E. Frequent expression of haemopoietic and non-haemopoietic antigens by neoplastic plasma cells: an immunohistochemical study using formalin-fixed, paraffin-embedded tissue. *Histopathology* 1992; 20: 35–40.

DOI: 10.1097/PAT.0b013e328359fba6

Expression of oxytocin and its receptor in healthy and varicose great saphenous veins

Sir,

Primary varicosis affects up to 40% of men and up to 51% of women. Risk factors are Western lifestyle, hormonal changes, genetics, age, female gender, parity, adipositas and standing occupation.[1–3] However, little is known about its pathophysiology. Contradicting theories range from abnormalities in the valve structures to functional and morphological changes of the vein wall as well as abnormal extracellular matrix organisation.[4,5] Oxytocin (OT), which has its well-established roles in obstetrics and gynecology, induces smooth muscle contractions. Rhythmic contractions occur on stimulation with OT in whole swine uteri,[6] the vaginal wall in the rabbit[7] and in human myometrium.[8] Binding of OT to its Gq coupled OT receptor (OTR) initiates various transduction cascades causing direct cell contraction via rhoA and the indirect cGMP-NO pathway.[9] In addition to its role during pregnancy, OT also has a general cardiovascular function in both genders.[10] The hormone and its receptor are primarily synthesised in the hypothalamus but also in the cardiovascular system and in peripheral vessels.[10] In detail, OT cardiovascular actions include natriuresis, blood pressure reduction, negative inotropic and chronotropic effects, parasympathetic neuromodulation as well as vasodilatation triggered by the NO pathway that is also involved in endothelial cell growth and anti-inflammatory activity.[11] In this study we analysed the expression of OT and OTR in control and incompetent great saphenous veins (GSVs) in order to define a potential pathophysiological role of OT in primary chronic venous insufficiency.

The ethic committee of the University of Tuebingen approved the investigation protocol. Every patient signed

Copyright © Royal College of pathologists of Australasia. Unauthorized reproduction of this article is prohibited.

an informed consent form in accordance with the Declaration of Helsinki principles prior to surgery. Detailed information on patients and tissues is provided in the supplementary Materials and Methods section (http://links.lww.com/PAT/A6).

During stripping surgery, 5–10 cm proximal samples of incompetent GSVs without relation to different sites of dilatation were obtained; from five incompetent GSVs, proximal and distal samples were used. For histological analysis, the tissues were fixed in 4°C buffered paraformaldehyde for 24 h before paraffin embedding. Serial sections of 3 μm were cut, mounted onto polylysin-coated slides and stained with H&E for histological evaluation.

The primary antibodies in this study were anti-human oxytocin (1:2000, rabbit polyclonal, ab2078; Abcam, UK) and anti-oxytocin receptor (1:100, rabbit polyclonal, ab13051; Abcam), automatically stained after standard protocols. Negative control sections were produced by omission of the primary antibody and did not show any staining, while the positive control slides (human endometrium and myometrium; Fig. 1A) were stained with the primary antibody showing no background reaction. We immunohistochemically processed and digitised 21 healthy and 41 varicose GSVs using an Axioplan 2 microscope (Carl Zeiss, Germany) with a mounted digital camera (Zeiss AxioCam color; Carl Zeiss). Slides were randomly analysed by two examiners blinded to the clinical diagnosis. A semi-quantitative staining four-step score was established (–, no expression; +, low expression; ++, moderate expression; +++, strong expression; Fig. 1B). We did not detect a significant inter-observer variability using this scoring technique. For statistical analysis, two groups of samples were clustered: – and + (low expression), versus ++ and +++ (strong expression). Analysis was performed with Fisher's exact test. p values <0.05 were considered significant.

Fig. 2 and 3 show expression of OT (Fig. 2) and OTR (Fig. 3) in healthy and incompetent great saphenous veins. In the healthy GSVs, OT was abundantly expressed in endothelial cells, the tunica media (i.e., the muscular layer of the vein wall; Fig. 2A,B) and in similar compartments of the vasa vasorum of the adventitia (small nutrient arteries and veins in the external vein wall; Fig. 2C). Further, OT was detected in small nerve fibres in the adventitia (Fig. 2D). A corresponding, but lower expression of the OTR was detected in the tunica media (Fig. 3A,B), vasa vasorum (Fig. 3C) and in endothelial cells (Fig. 3D) of the healthy GSVs.

In the incompetent GSVs, the principal expression pattern of OT and OTR was similar to the healthy GSVs. OT was expressed in endothelial cells, tunica media (Fig. 2E,F),

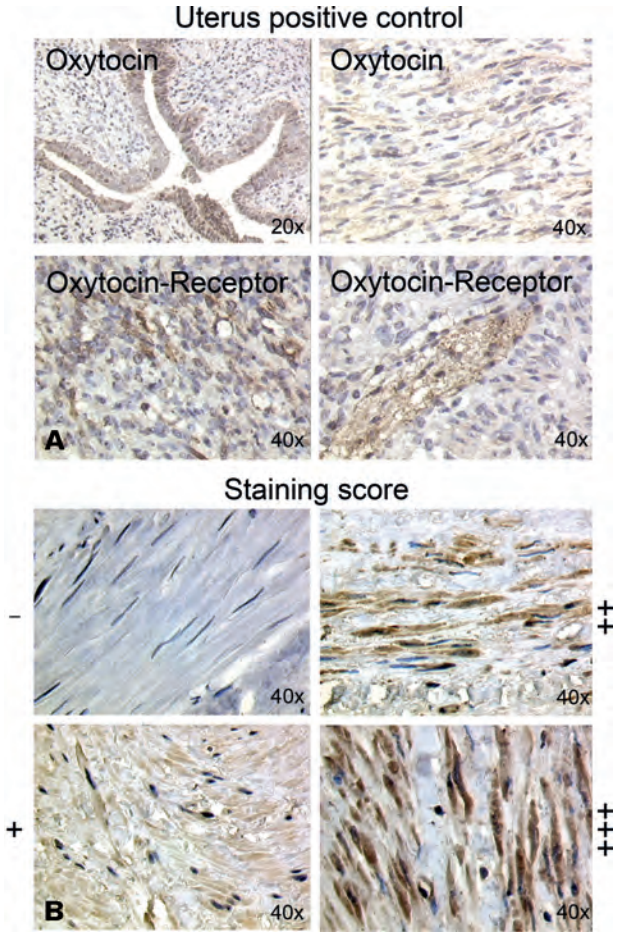

Fig. 1 Uterus positive staining controls and staining score. (A) Human uterus tissue served as positive control for OT (upper panel) and for OTR (lower panel). (B) Semi-quantitative staining score (–, +, ++, +++).

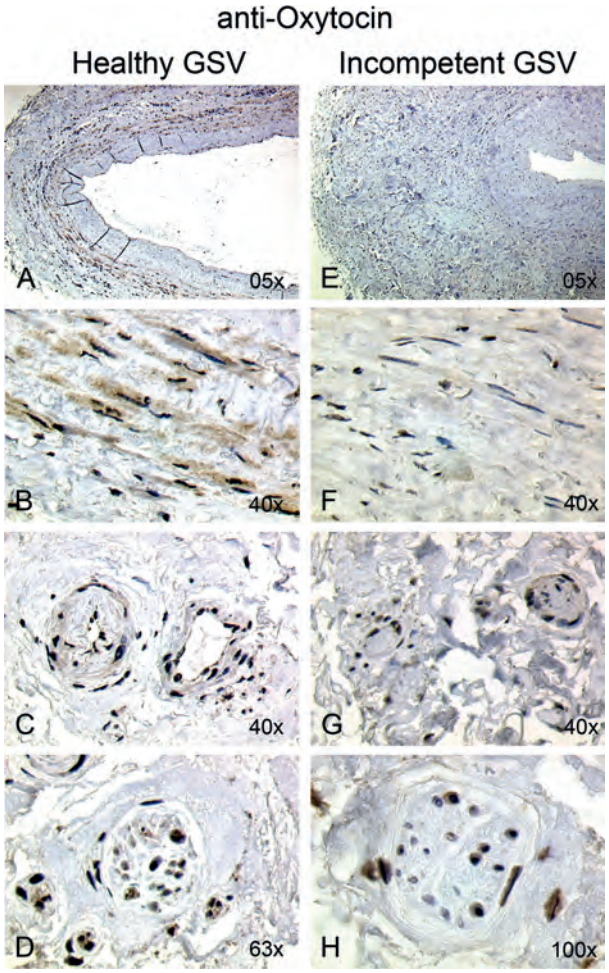

Fig. 2 Expression of OT in healthy and incompetent great saphenous veins. (A) Overview of a cross section of a healthy GSV, OT staining. The expression of OT can already be distinguished at 5× magnification. (B) At higher magnification, OT positive smooth muscle cells of the tunica media become visible. (C) OT expression in endothelial cells and smooth muscle cells of vasa vasorum. (D) Cross section of a small nerve fibre in the adventitia depicting OT positivity. (E) Overview of a cross section of an incompetent GSV. Hardly any expression of OT in the tunica media can be distinguished at 5× magnification. (F) At higher magnification single smooth muscle cells show low expression of OT. (G,H) In the adventitia nerve fibres also stain positive for OT.

Copyright © Royal College of pathologists of Australasia. Unauthorized reproduction of this article is prohibited.

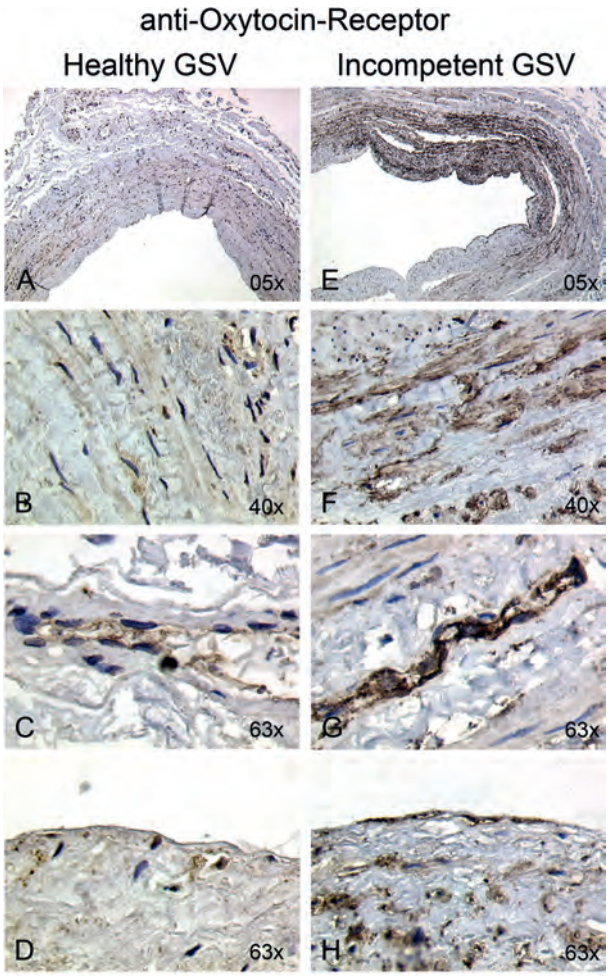

	GSV ++/+++	GSV -/+	Incompetent GSV ++/+++	Incompetent GSV -/+	p-value*
Anti-OT	8/21	13/21	6/41	35/41	<0.05
Anti-OTR	1/20	19/20	19/41	22/41	<0.05

Fig. 3 Expression of OTR in healthy and incompetent great saphenous veins. (A) Overview of a cross section of a healthy GSV, OTR staining. Low expression of OTR can already be distinguished at 5× magnification. (B) At higher magnification, OTR positive smooth muscle cells of the tunica media become visible. (C) OTR expression in the vasa vasorum. (D) Endothelial cells with weak expression of the OTR. (E) Overview of a cross section of an incompetent GSV. High expression of the OTR in the tunica media can be distinguished already at 5× magnification. (F) At higher magnification, single smooth muscle cells in the tunica media show strong expression of the OTR. (G,H) Both the endothelial cells of the vasa vasorum in the adventitia and the endothelium of the GSV show a strong positivity for the OTR. (I) Statistical analysis of expression intensity of OT and OTR. *Fisher's exact test.

vasa vasorum (Fig. 2G) and in small nerve fibres in the adventitia (Fig. 2H). OTR was also expressed in the tunica media (Fig. 3E,F), vasa vasorum (Fig. 3G) and in endothelial cells (Fig. 3H) of the incompetent GSVs. Evaluation of proximal and distal samples of the same incompetent GSV showed no differences in expression of OT and OTR (not shown). We did not detect gender-specific and age-specific differences in expression of OT and OTR. Evaluation was performed by comparing low expression (−/+) with strong expression (++/+++) intensity (Fig. 3I). The expression level of OT differed in both groups. In the tunica media, expression of OT was decreased in incompetent compared with healthy GSVs. There was a strong expression in six of 41 incompetent GSVs compared with eight of 21 in the healthy GSVs ($p < 0.05$, Fisher's exact test). The expression of the OTR was inversely distributed; strong in incompetent GSVs, but almost absent in healthy GSVs in the tunica media (strong expression 19/41 versus 1/20; $p < 0.05$, Fisher's exact test). Corresponding staining intensities were detected in the vasa vasorum.

So far, descriptive reports on differences, e.g., in collagen or matrix metalloproteinase (MMP) expression[12] in healthy and incompetent GSVs have been published. In the latter study, human thymic smooth muscle cells were analysed for MMP-2 expression and gelatinase activity under experimentally-induced cyclic stretch as a surrogate for smooth muscle cells from the tunica media of the GSV.[12] The aim of our study was to analyse the expression of OT and its receptor OTR in healthy and incompetent GSVs. Our data showed that the expression of OT is decreased, while the expression of the OTR is increased in incompetent GSVs. Our results propose OT as a molecule that might play a role in the pathophysiology of primary chronic venous insufficiency, possibly by regulating the contraction tonus of the venous wall.

Our findings suggest an OT system in peripheral veins which goes along with published data on peripheral arterial vascular effects of OT influencing blood pressure in animals.[10] In rats, the cardiac OT system is implicated in cardiovascular responses to stress; post-natal treatment with OT was able to decrease blood pressure in spontaneously hypertensive adult male rats.[9] The expression patterns of OT and ORT in GSVs as described in this study are in line with the published data showing that OT effects the contraction tonus of cardiac cells and smooth muscle cells in the cardiovascular system and in the uterus during labour induction.[10,11] The venous tunica media is less developed than its counterpart in the arterial system, where it regulates the blood pressure via contraction. The expression of OT in the same compartment of the venous system implies a similar contractile function. Therefore, this observation suggests that the blood return from the lower extremities might in part be conducted by contraction of the GSV in addition to the calf muscle pump and competent valves (providing unidirectional blood flow towards the heart). Our results demonstrated a reduced expression of OT in incompetent GSVs, suggesting a chronically reduced contractile capacity of the vein wall which might contribute to incomplete closure of the venous valves. This might be responsible in part for the chronic dilatation of the entire vein leading to primary venous insufficiency. Further, our results show that the expression of the OTR was increased in endothelial cells and in smooth muscle cells of the tunica media of incompetent GSVs. This suggests a positive, up-regulating feedback mechanism to maintain a contractile function of the vein wall. Obviously, it is not clear whether the different expression of OT and OTR observed in the incompetent GSVs are secondary changes that develop after the varicosities have developed. In conclusion, our results suggest that the decreased expression of oxytocin in the tunica media of incompetent GSVs might contribute to the pathophysiology of primary venous insufficiency, thus representing a possible novel candidate for pharmacological treatment.

Acknowledgements: We would like to thank Annemarie Adam (Department of Pathology, University of Tuebingen) for paraffin sections and immunohistochemistry.

Conflicts of interest and sources of funding: This work was supported by a research grant to CB by the Deutsche Gesellschaft fuer Phlebologie [German Phlebological Society]. The authors declare no financial conflict of interest.

Copyright © Royal College of pathologists of Australasia. Unauthorized reproduction of this article is prohibited.

Sarah Schott*†
Julia Adams‡
Arno Bern§
Claus Garbe‡
Christian Busch‡

**Department of Gynecology and Obstetrics, University of Heidelberg, †Institute of Pathology, and ‡Department of Dermatology, University of Tuebingen, and §Practice Clinic of Phlebology, Tuebingen, Germany*

Contact Dr C. Busch.
E-mail: Christian.Busch@med.uni-tuebingen.de

1. Somers P, Knaapen M. The histopathology of varicose vein disease. *Angiology* 2006; 57: 546–55.
2. Meissner MH, Moneta G, Burnand K, *et al*. The hemodynamics and diagnosis of venous disease. *J Vasc Surg* 2007; 46 (Suppl S): 4S–24S.
3. Meissner MH, Gloviczki P, Bergan J, *et al*. Primary chronic venous disorders. *J Vasc Surg* 2007; 46 (Suppl S): 54S–67S.
4. Elsharawy MA, Naim MM, Abdelmaguid EM, *et al*. Role of saphenous vein wall in the pathogenesis of primary varicose veins. *Interact Cardiovasc Thorac Surg* 2007; 6: 219–24.
5. Travers JP, Brookes CE, Evans J, *et al*. Assessment of wall structure and composition of varicose veins with reference to collagen, elastin and smooth muscle content. *Eur J Vasc Endovasc Surg* 1996; 11: 230–7.
6. Dittrich R, Mueller A, Oppelt PG, *et al*. Differences in muscarinic-receptor agonist-, oxytocin-, and prostaglandin-induced uterine contractions. *Fertil Steril* 2009; 92: 1694–700.
7. Aughton KL, Hamilton-Smith K, Gupta J, *et al*. Pharmacological profiling of neuropeptides on rabbit vaginal wall and vaginal artery smooth muscle in vitro. *Br J Pharmacol* 2008; 155: 236–43.
8. Gullam JE, Blanks AM, Thornton S, *et al*. Phase-plot analysis of the oxytocin effect on human myometrial contractility. *Eur J Obstet Gynecol Reprod Biol* 2009; 144: 20–4.
9. Viero C, Shibuya I, Kitamura N, *et al*. Oxytocin: Crossing the bridge between basic science and pharmacotherapy. *CNS Neurosci Ther* 2010; 16: e138–56.
10. Gutkowska J, Jankowski M, Mukaddam-Daher S, *et al*. Oxytocin is a cardiovascular hormone. *Braz J Med Biol Res* 2000; 33: 625–33.
11. Gutkowska J, Jankowski M. Oxytocin revisited: It is also a cardiovascular hormone. *J Am Soc Hypertens* 2008; 2: 318–25.
12. Feldner A, Otto H, Rewerk S, *et al*. Experimental hypertension triggers varicosis-like maladaptive venous remodeling through activator protein-1. *FASEB J* 2011; 25: 3613–21.

DOI: 10.1097/PAT.0b013e328359fbce

Purple bowel discovered at autopsy

Sir,

Bowel discolouration due to ingested material is an unusual finding at autopsy, which may occasionally be a source of confusion. We present a case of bowel discolouration due to beetroot in an otherwise routine autopsy.

Our patient was a 66-year-old male farmer who died unexpectedly of severe triple vessel coronary artery disease. An autopsy was performed 6 days following death. In addition to the cardiac abnormalities it was noted that the small bowel, some segments of the large bowel and rectum were dull purple in colour (Fig. 1 and 2). Of specific note was that the mesenteric fat was of normal colour and appearance, and the absence of significant amounts of peritoneal fluid. The bowel did not have any macroscopic evidence of serosal inflammation. A number of causes for the discolouration were considered, including blunt trauma, vascular compromise due to volvulus, ingestion of toxic substances, and metabolism of bowel content by enteric bacteria. Opening the small bowel revealed it was packed with obvious beetroot fragments (Fig. 3).

Fig. 1 A loop of small bowel displaying the purple colour, with attached normal mesenteric fat.

The distinctive red-purple colour of beetroot (*Beta vulgaris*) is due to a class of pigments called betalains. Once ingested, they are inherently unstable and their absorption is dependent on a number of physiological factors.[1–3] After absorption they are essentially unmodified by first-pass metabolism and rapidly cleared in the urine.[4] Unabsorbed pigment is excreted with faeces.[3]

Given the widespread availability of beetroot it is perhaps more surprising that bowel discolouration is not noted with greater frequency, especially during surgery and endoscopic procedures. A literature search reveals only two published cases, both in a post-mortem setting.[5,6] There are a number of possible explanations. Firstly, it is unknown how much beetroot is required to produce this discolouration. Secondly, as noted above, the absorption and excretion of betalains is highly variable and dependent on a number of physiological factors. When combined with preprocedural fasting, the colour changes are unlikely to be observed in a living patient. Thirdly, sufficient time must elapse between death and autopsy for mucosal autolysis to occur, which allows the pigments to diffuse to the serosa. In our patient, the discolouration of the intestines was an incidental finding consistent with passive diffusion of beetroot pigments, presumably due to the large volume of beetroot present and the extended length of time between death and performance of the autopsy.

Fig. 2 Rectum (right) showing similar purple discolouration.

Copyright © Royal College of pathologists of Australasia. Unauthorized reproduction of this article is prohibited.

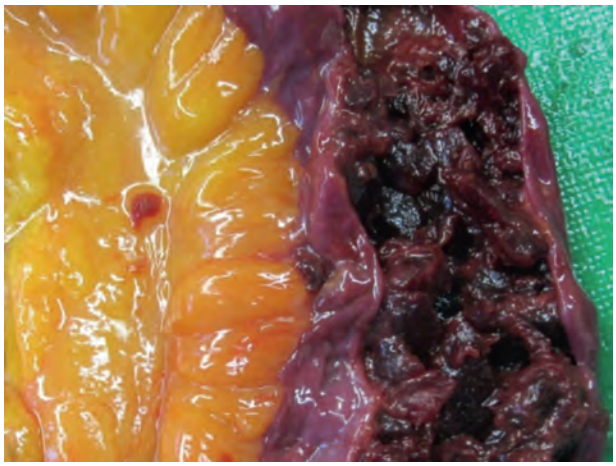

Fig. 3 Small bowel contents, with beetroot fragments clearly visible.

Beetroot is a rare cause of bowel discolouration in the post-mortem setting. The presence of undigested fragments within the bowel lumen is normally obvious; however, due to increased availability and popularity of concentrated beetroot supplements (in powder, capsule or juice form), pathologists are well served to remember this possibility when confronted with a purple bowel of no obvious cause.

Conflicts of interest and sources of funding: The authors state that there are no conflicts of interest to disclose.

Cheng Liu*
Peter Smart†

**Healthscope Pathology, Bella Vista, and †Healthscope Pathology, Wagga Wagga, NSW, Australia*

Contact Dr C. Liu.
E-mail: johnliu1985@hotmail.com

1. Mitchell SC. Food idiosyncrasies: Beetroot and asparagus. *Drug Metab Dispos* 2001; 29: 539–43.
2. Watson WC, Luke RG, Inall JA. Beeturia: its incidence and a clue to its mechanism. *Br Med J* 1963; 2: 971–3.
3. Eastwood MA, Nyhlin H. Beeturia and colonic oxalic acid. *QJM* 1995; 88: 711–7.
4. Watts AR, Lennard MS, Mason SL, *et al*. Beeturia and the biological fate of beetroot pigments. *Pharmacogenetics* 1993; 3: 302–11.
5. Klug E, Maxeiner H. Unusual coloration of intestinal contents. A surprising observation and its harmless explanation. *Arch Kriminol* 1981; 168: 129–32.
6. Cserni G, Kocsis L. The case of the purple colon. *Virchows Arch* 2008; 452: 703.

DOI: 10.1097/PAT.0b013e328359e167

Positive and negative interference in immunoassays following biotin ingestion: a pharmacokinetic study

Sir,
We read with interest the recent report on biotin interference on thyroid stimulating hormone (TSH) and free thyroid hormone (fT4 and fT3) measurement by Kwok and colleagues,[1] which was similar to a case we reported previously.[2] Here, we would like to share our further experience of both positive and negative interference on a range of different immunoassays using different analytical systems and the time response curve following ingestion of biotin.

Our index patient was a 1-week-old baby born with features of liver failure and lactic acidosis who has been treated with biotin 30 mg per day (10 mg 8 hourly) since day 2 of life. At 1 week of age his thyroid function test (TFT) results on a Beckman DxI analyser (Beckman Coulter, USA) were: fT4 >77.7 pmol/L (reference interval 25–70), fT3 24.9 pmol/L (3.8–6.0) and TSH 3.75 mU/L (1.0–25.0). The discordant TFT pattern prompted further investigations to exclude assay interference. There was no change in results after treatment with Scantibodies (heterophile antibody blocking agent; Scantibodies Laboratory, USA). Furthermore, TFT results were normal when measured on Abbott Architect (Abbott, USA) and Siemens Centaur (Siemens, Germany) analysers, confirming assay interference specific to our Beckman DxI analyser. All results were reproducible at 1 month and 6 weeks of age. Biotin was then discontinued and all TFT results rapidly normalised.

To confirm the biotin interference in immunoassays and to examine the kinetics of the interference, one of the authors ingested 30 mg of biotin and blood samples were collected at 0, 1, 2, 4, 8 and 25 h following ingestion. Serum specimens were tested on Beckman DxI for fT4, fT3 and thyroglobulin, Abbott Architect analyser for fT4 and fT3, and Roche E170 (Roche, Switzerland) for DHEAS, oestradiol, testosterone and ferritin.

Our results showed that in competitive immunoassays based on biotin-streptavidin interaction, excess biotin in the specimen competes with the biotinylated analog for the binding sites on streptavidin resulting in falsely high values. This can be seen with fT4 and fT3 assays (Fig. 1A) on Beckman DxI. Testosterone, DHEAS and oestradiol on Roche E170 showed a similar pattern (data not shown). When the principle of biotin-streptavidin interaction is applied in the sandwich assay format, excess biotin in the sample displaces biotinylated antibodies resulting in falsely low results. This can be seen with the Beckman thyroglobulin (Fig. 1B) and the Roche E170 ferritin assays (data not shown). No interference was seen on the Abbott Architect fT4 and fT3 assays as biotin-streptavidin interaction was not used in the assay format.

The time response curve revealed that the interference peaked around 2 h post-biotin ingestion for all the analytes we measured. The effect lasted for approximately 5 h for DHEAS, oestradiol, testosterone and ferritin. However, interference for fT4, fT3 and thyroglobulin on Beckman DxI endured for up to 24 h. The magnitude of change in concentration is different among the analytes. fT3, DHEAS and testosterone showed a maximum 3-fold increase while fT4 increased by 7-fold. Thyroglobulin levels were decreased by 11-fold, however ferritin level dropped by only 1.5-fold. The most exaggerated effect was seen in the Roche oestradiol assay with a 138-fold increase from the initial value.

As mentioned by Kwok and colleagues, the biotin interference in immunoassay is not expected with normal dietary intake of biotin. However, high doses of biotin (5–20 mg daily) are used in several conditions such as biotinidase deficiency and propionic acidaemia. Many over-the-counter vitamin supplements also contain significant amount of biotin per tablet, for example, Swisse Ultiboost Hair Skin Nails, 2.6 mg biotin; Nature's Own Balance Plus Glow Multivitamin, 2.5 mg biotin; and Blackmore's Nails Hair and Skin tablets, 1.3 mg biotin. The usual recommended dose of the

Copyright © Royal College of pathologists of Australasia. Unauthorized reproduction of this article is prohibited.

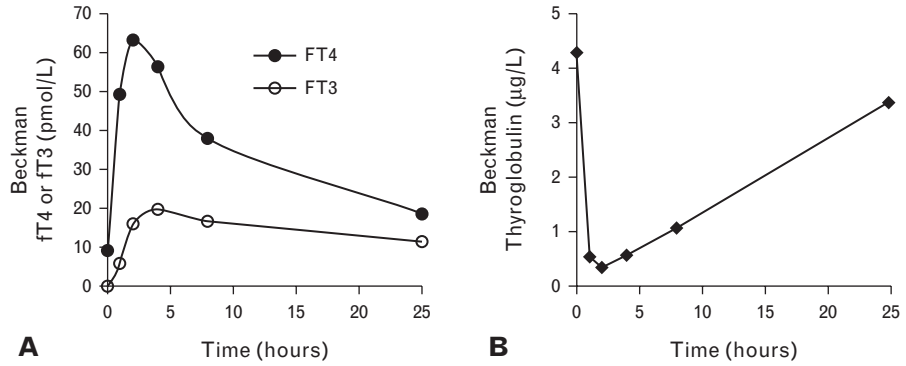

Fig. 1 Interference of the ingested biotin on (A) fT4 and fT3, and (B) thyroglobulin assays on Beckman DxI.

above vitamins are one tablet per day. Subtle effects could be expected with these doses, but more pronounced if patients took two or three tablets at once. Therefore pathologists need to be aware of the possibility of biotin interference in immunoassays and require clear understanding of the assay formats to detect and overcome these interferences.

Conflicts of interest and sources of funding: The authors state that there are no conflicts of interest to disclose.

Nilika G. Wijeratne*
James C. G. Doery*†
Zhong X. Lu*†

**Department of Pathology, Monash Medical Centre, Clayton, and †Department of Medicine, Monash University, Clayton, Vic, Australia*

Contact Dr N. G. Wijeratne.
E-mail: nilikaw@yahoo.com

1. Kwok JS-S, Chan IH-S, Chan MH-M. Biotin interference on TSH and free thyroid hormone measurement. *Pathology* 2012; 44: 278–80.
2. Wijeratne N, Doery JCG, Lu ZX. Pseudo-hyperthyroxinemia – uncommon cause of immunoassay interference due to biotin therapy. *Clin Biochem Rev* 2010; 31 (Suppl i): S34.

DOI: 10.1097/PAT.0b013e32835a3c17

Copyright © Royal College of pathologists of Australasia. Unauthorized reproduction of this article is prohibited.